Migrating and Non-migrating Tides in the MLT region

S. Miyahara
Kyushu University

2001 CEDAR-SCOSTEP Meeting
June 21, 2001
Longmont, Colorado

Contents of this talk

1. A brief review of theoretical background
   - •Definition of Migrating and Non-migrating tides
   - •Solutions of Laplace's tidal equation
     Hough Functions, Equivalent depth
   - •Sources of migrating tides
2. Examples of observed structure of tidal waves in the MLT region
   - •Migrating diurnal and semidiurnal tides
   - •Non-migrating tides
3. Dissipation of tides in the MLT region
   - •Eddy diffusion •Molecular diffusion
   - •Radiative cooling •Convective instability
   - •Gravity waves interaction
4. Excitation and propagation mechanisms of non-migrating tides
   - •Moist convective heating
   - •Tide-planetary waves interaction
   - •Effects of background mean zonal winds
5. Concluding remarks

Definition

Migrating tides

The phase propagates westward synchronized with the diurnal motion of the sun.

$$u \propto e^{i(n\sigma t + s\lambda)}, \qquad \sigma = \frac{2\pi}{1 \text{ solar day}},$$

n=s=1 (diurnal), and n=s=2 (semi-diurnal)

Non-migrating tides

The phase propagates westward or eastward, but not synchronized with the diurnal motion of the sun, or zonally homogeneous oscillation.

$$u \propto e^{i(n\sigma t + s\lambda)}, \qquad \sigma = \frac{2\pi}{1 \text{ solar day}},$$

n=1 (diurnal), and n=2 (semi-diurnal)

$s = 0, \pm 1, \pm 2, \pm 3, \cdots$

$s \neq 1$ (diurnal), and $s \neq 2$ (semi-diurnal)

Migrating diurnal tide, October

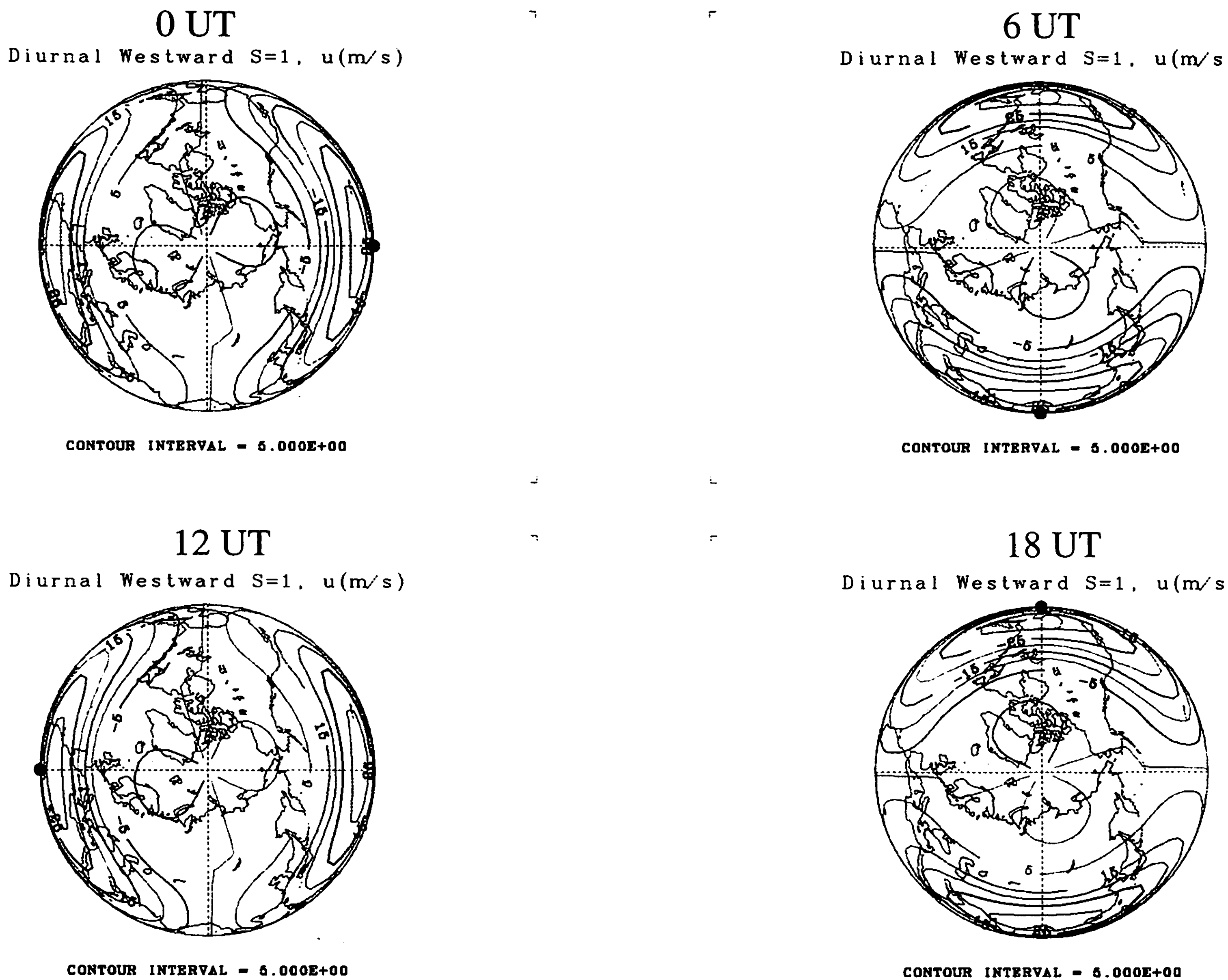

Diurnal westward moving S=1, u(m/s) z = 98 km

Nonmigrating diurnal tide, October

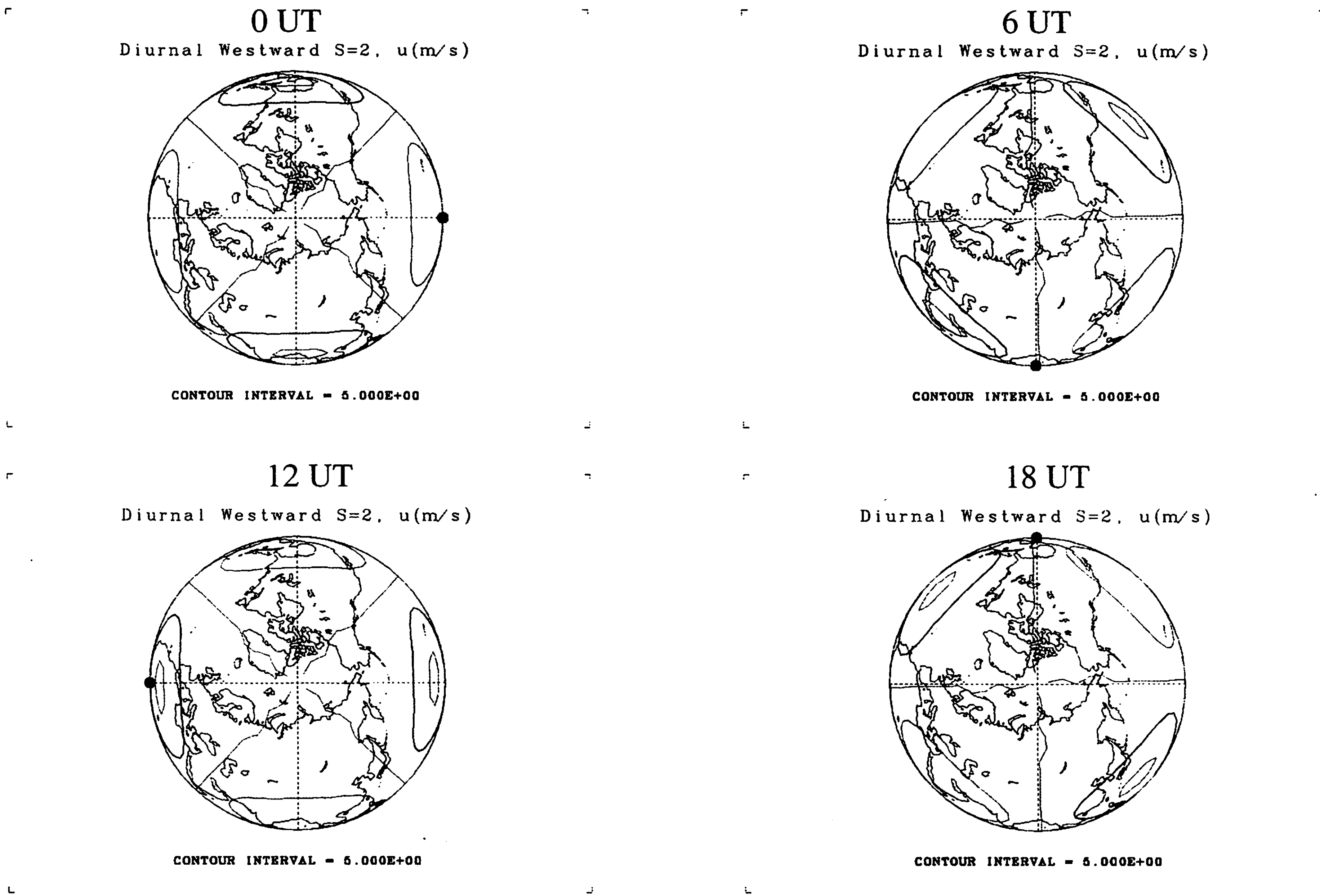

Diurnal westward moving S=2, u(m/s) z = 98 km

Migrating and nonmigrating diurnal tides, October

0 UT

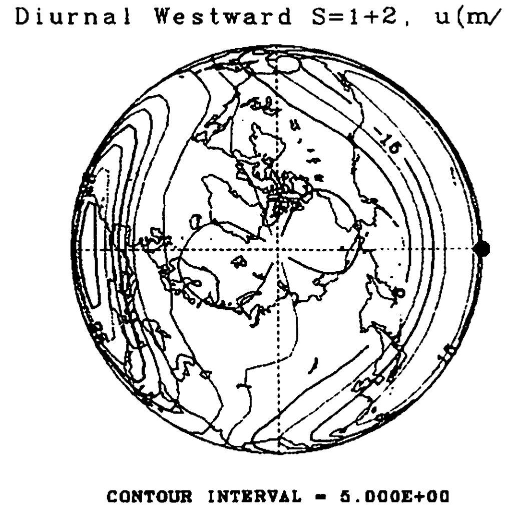

6 UT

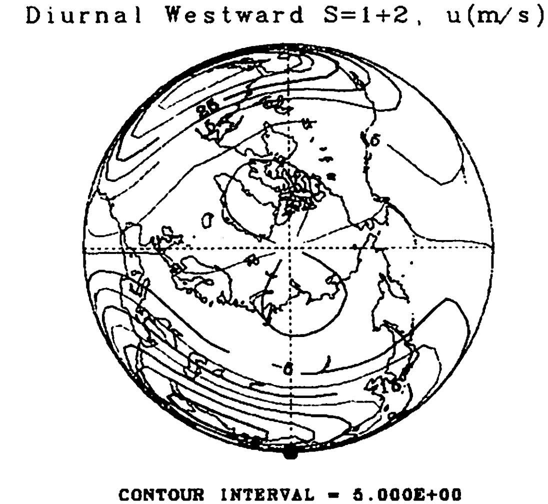

12 UT

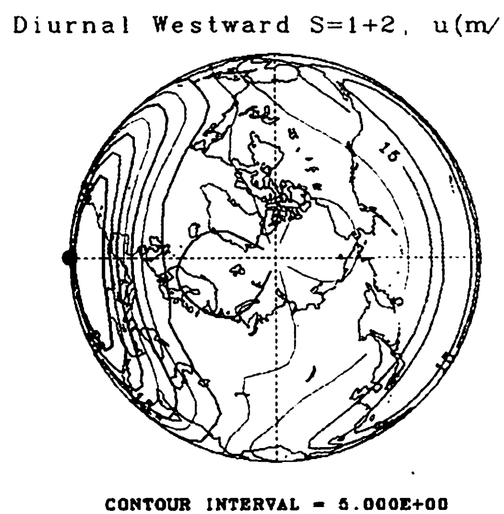

18 UT

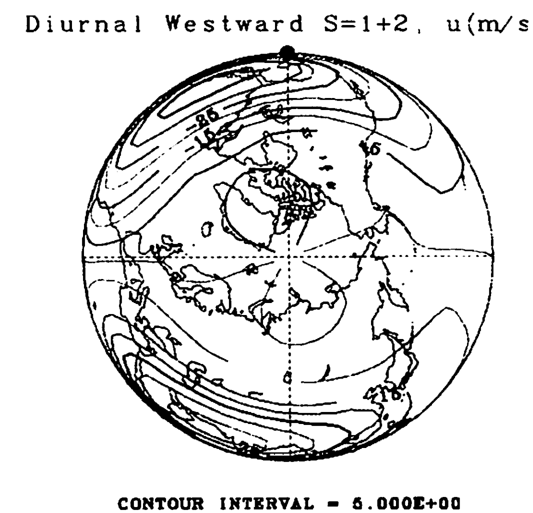

Diurnal westward moving S=1+2, u(m/s) z = 98 km

Migrating semidiurnal tide, October

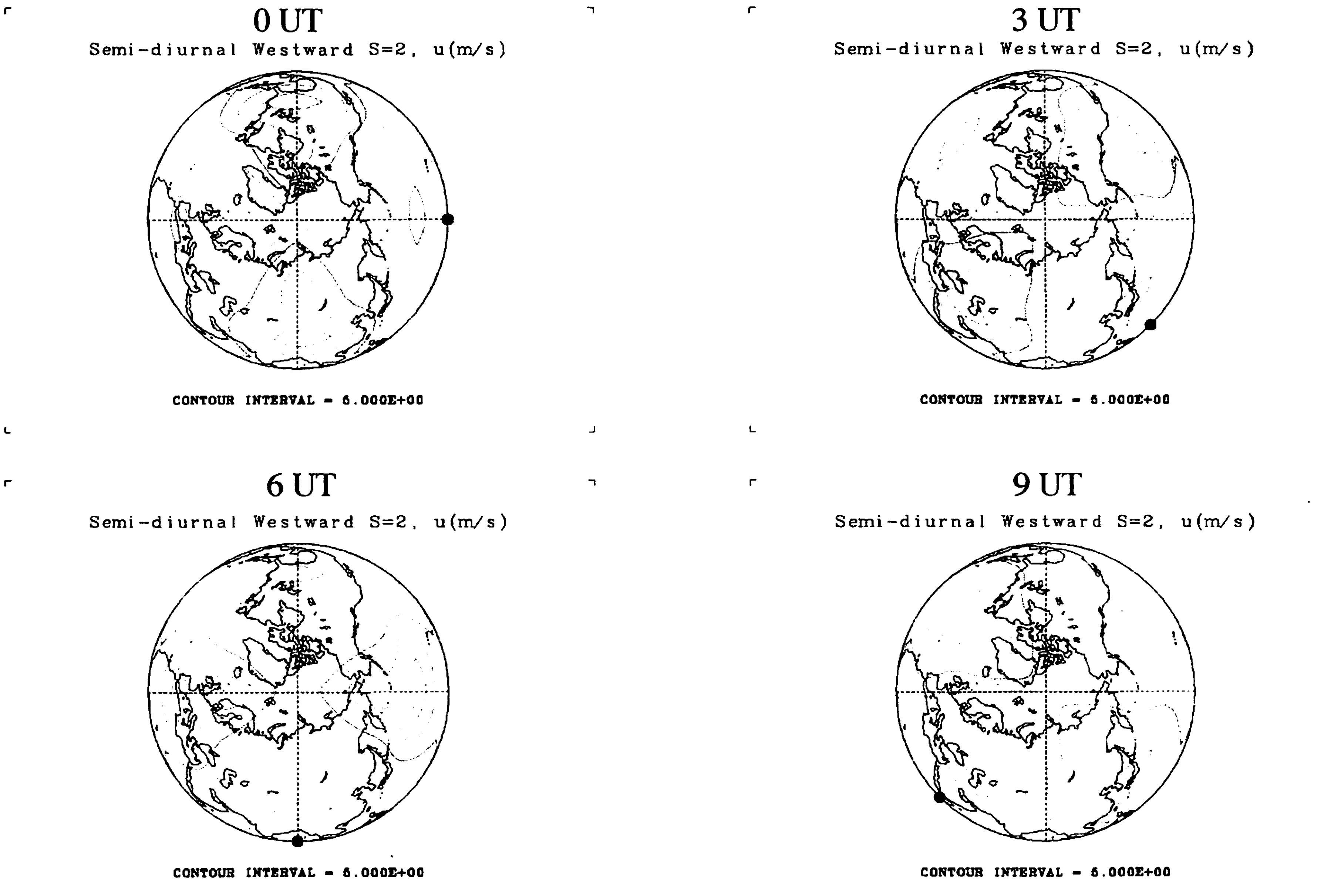

Semidiurnal westward moving S=2, u(m/s) z = 98 km

Non-migrating semidiurnal tide, October

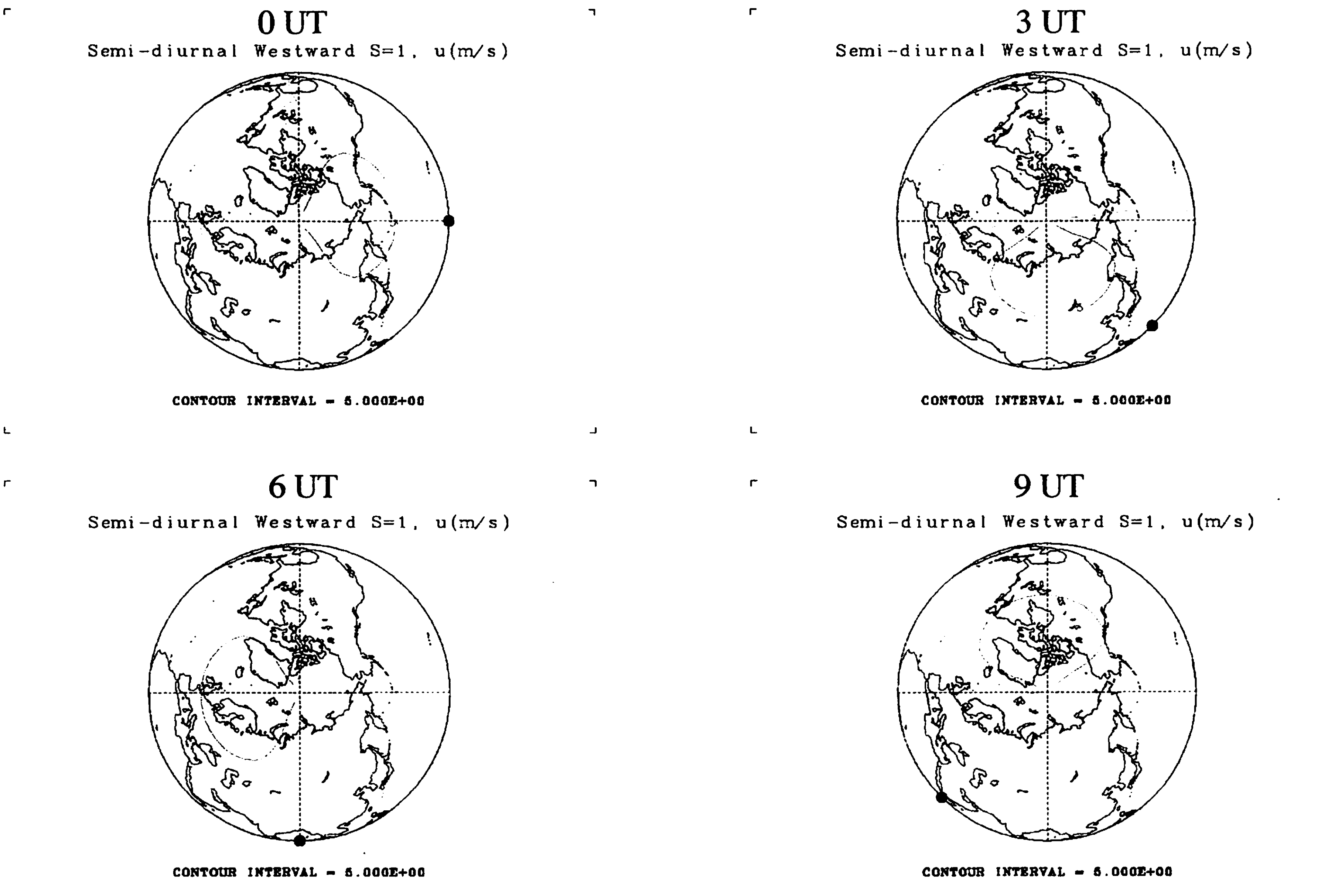

Semidiurnal westward moving S=1, u(m/s) z = 98 km

Migrating and non-migrating semidiurnal tides

0 UT

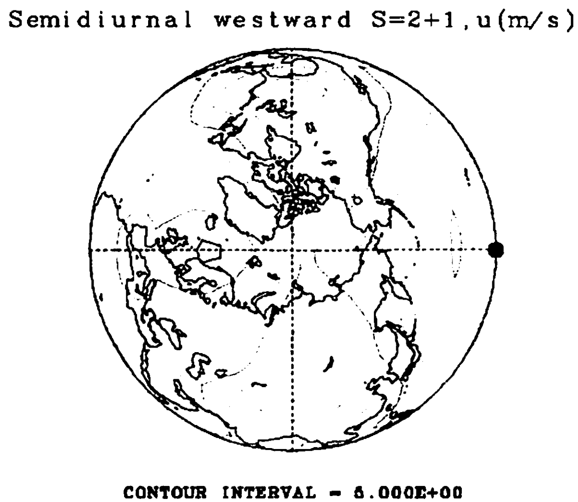

3 UT

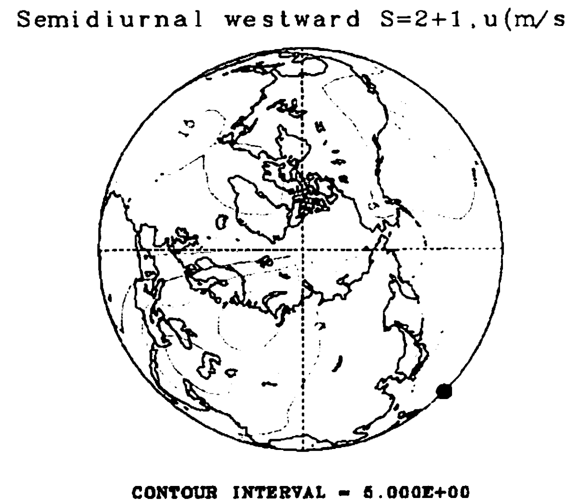

6 UT

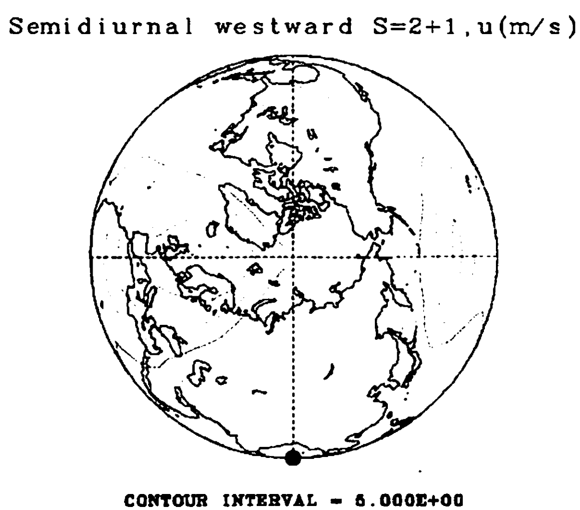

9 UT

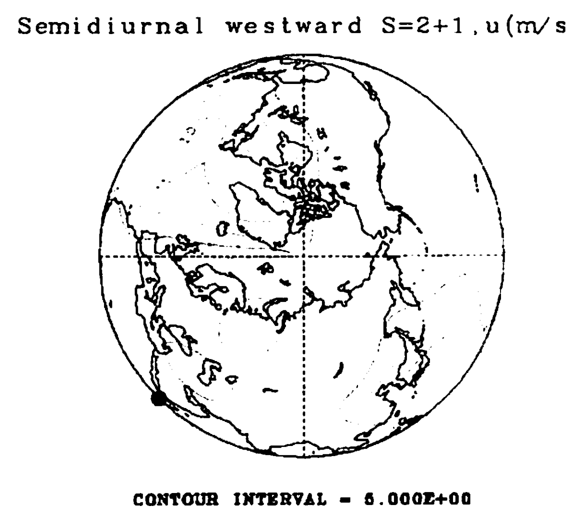

Semidiurnal westward moving S=2+1, u(m/s) z = 98 km

Longuet-Higgins (1967)

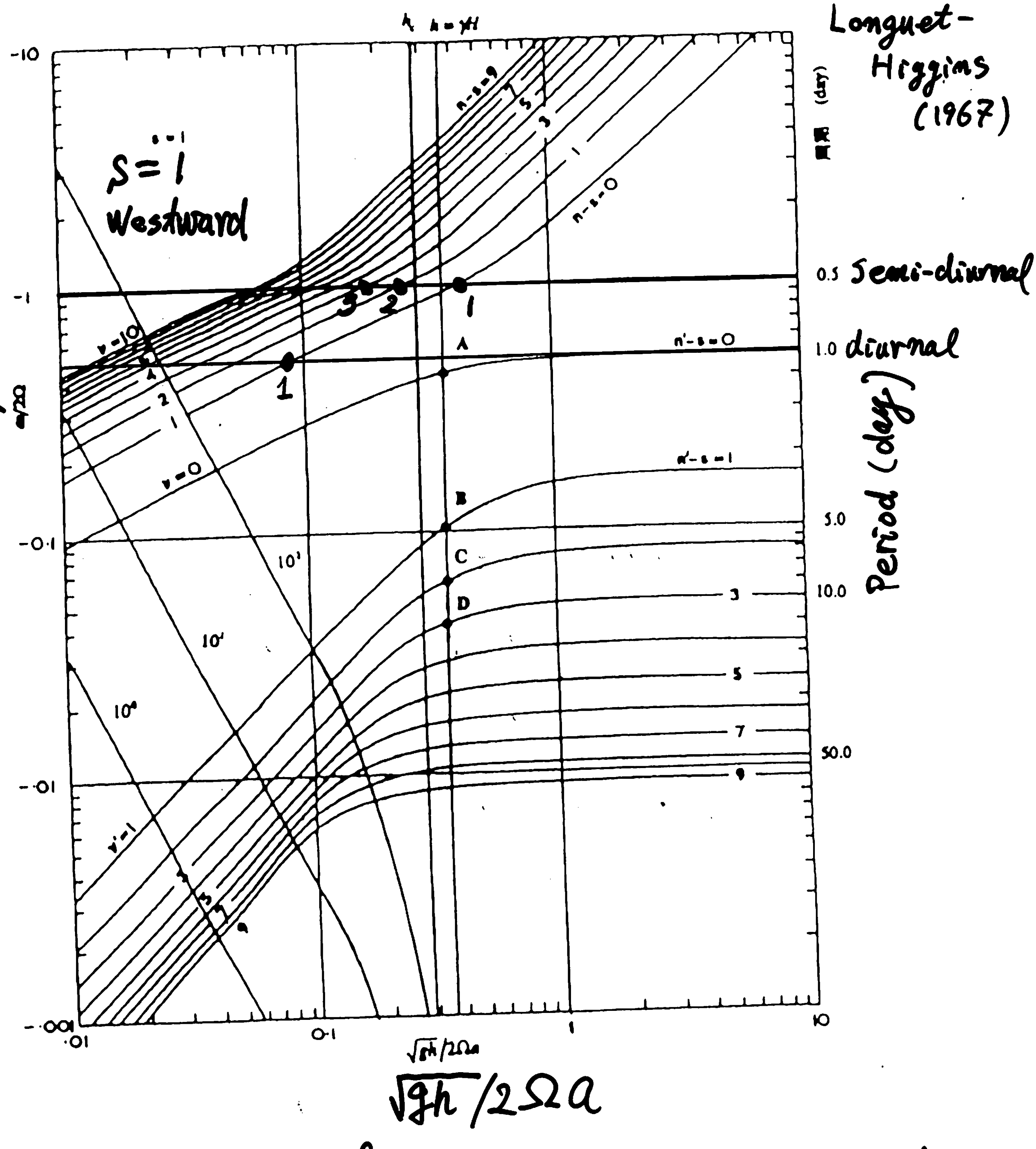

h : Equivalent depth

Vertical wave length $\lambda = \left(\sqrt{\frac{\kappa}{hH} - \frac{1}{4H^2}}\Big/2\pi\right)^{-1}$

$H = \frac{RT}{g}$: Scale height.

$\lambda_1 \sim 25 \sim 30$ km

λ_1 : N.P.

$\lambda_2 \sim 130$ km

$\lambda_3 \sim 80$ km

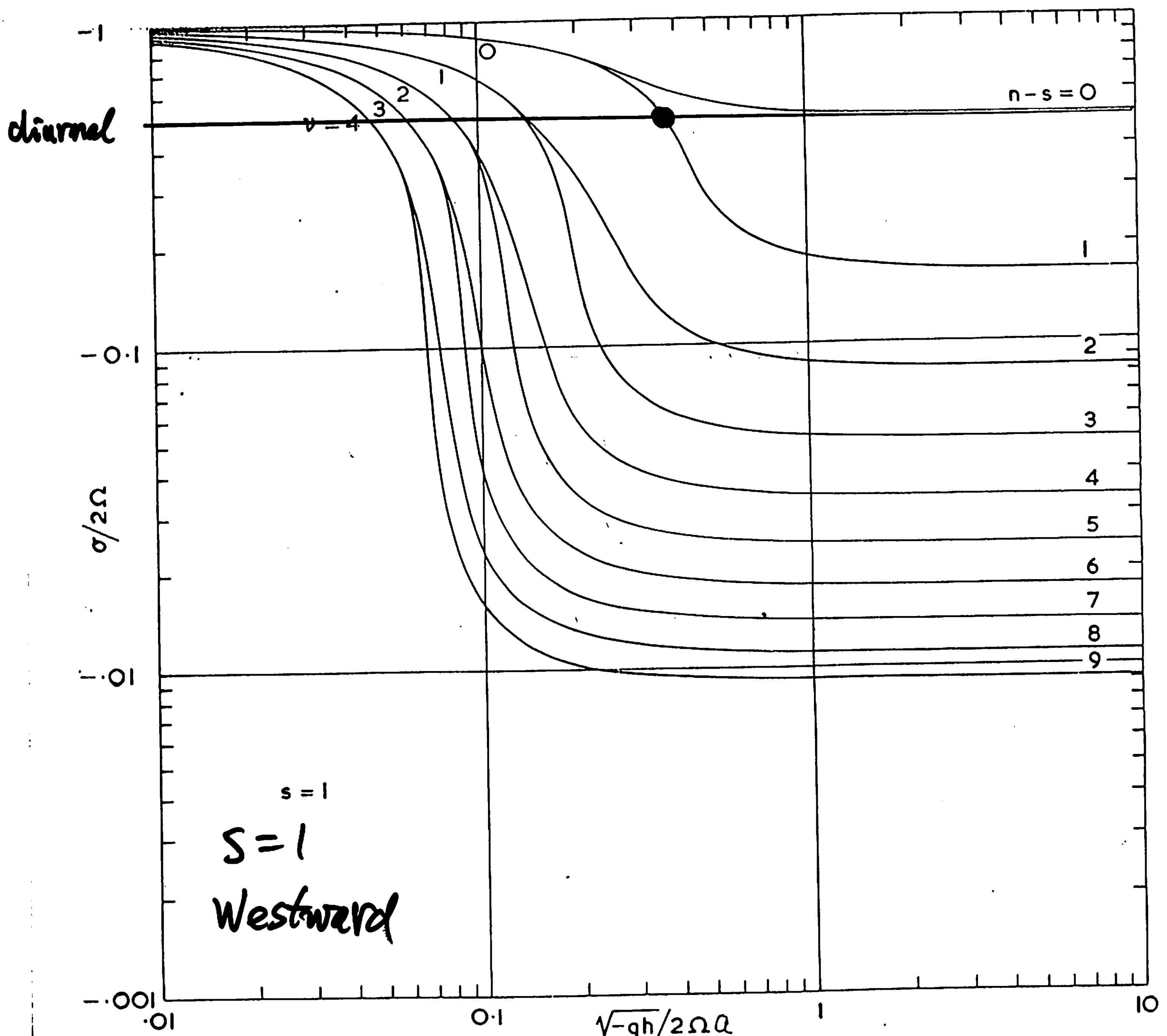

h<0

λ: N.P.

Figure 17b.

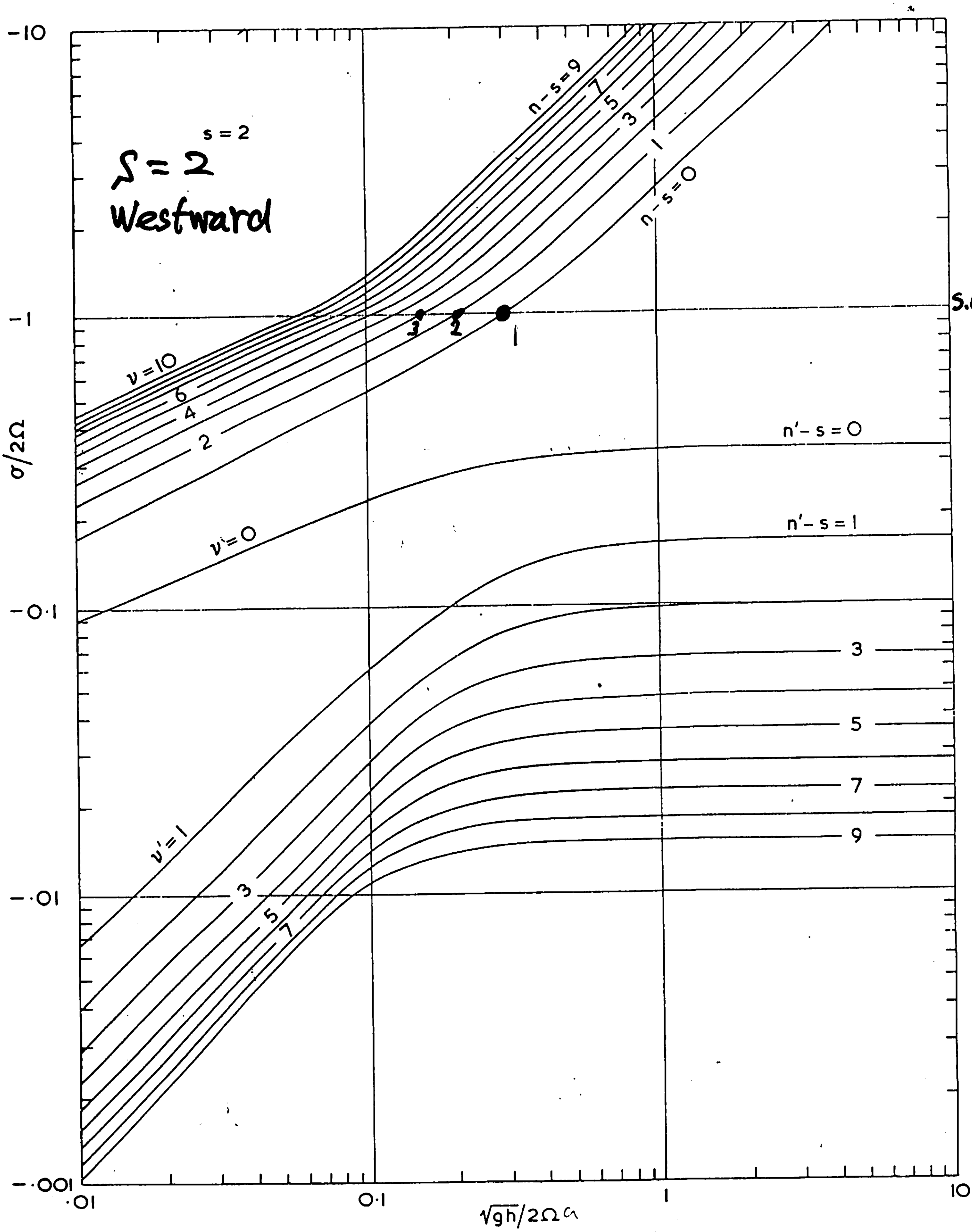

$\lambda_1 \sim 340$ km

Figure 36.

$\lambda_2 \sim 50$ km

$\lambda_3 \sim 30$ km

Forbes (1996)

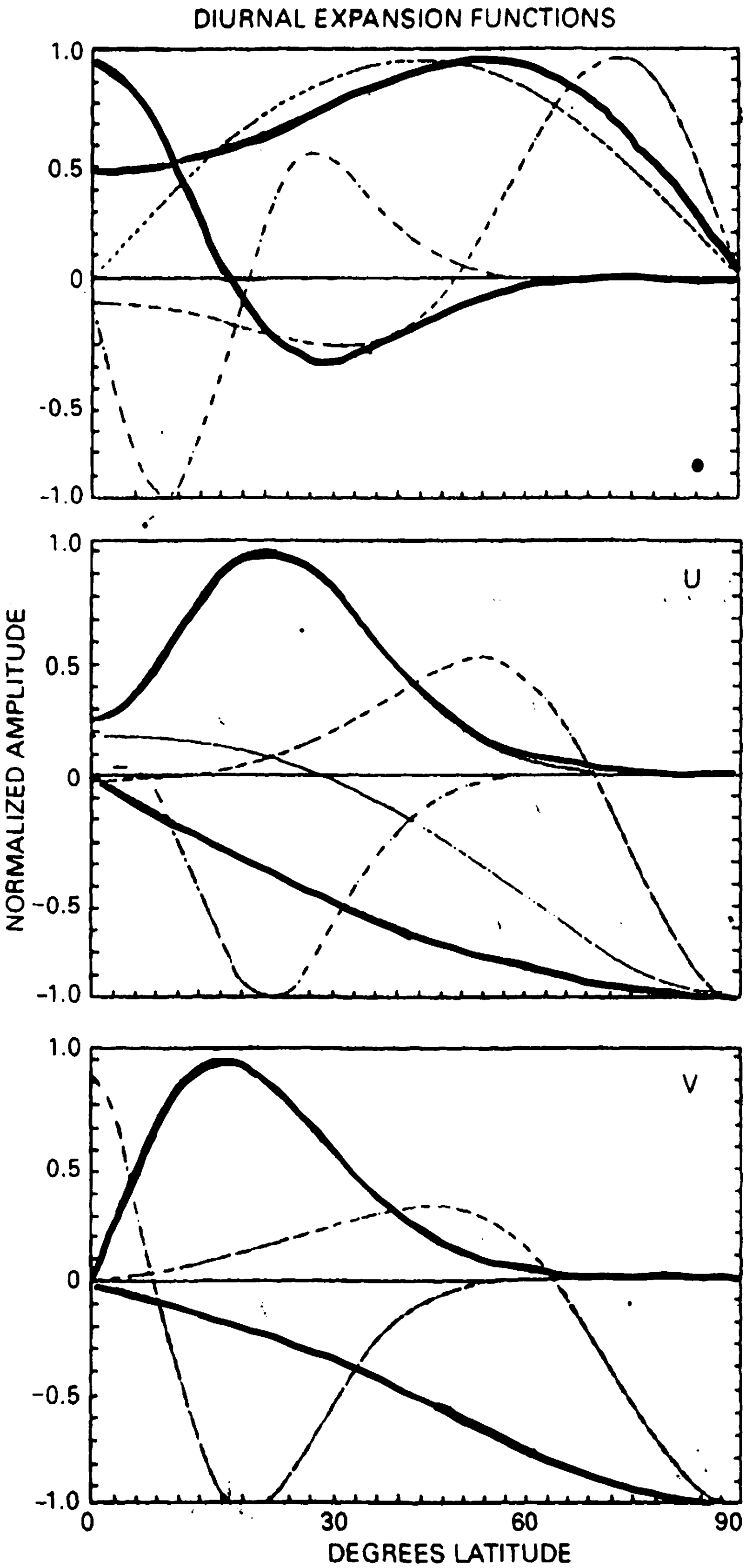

— (1, 1)
h = 0.691 km

— (1, -2)
h = -12.27 km

Fig. 1. *Top* Hough functions for diurnal modes normalized to a maximum value of unity. Keys and normalization factors for each Hough mode are as follows. (1,1) *solid line*, 0.606; (1, 1) *dashed line*, 1.034; (1, -2) *dotted line*, 1.054; (1, 4) *dashed-dotted line*, 0.513, (1,2), *dashed-double dotted line*, 0.641 *Bottom* Northerly velocity expansion functions for diurnal modes normalized to a maximum value of unity. Normalization factors are 0.026, 0.126, 0.100, 0.024, and 0.015, respectively. *Center* Westerly velocity expansion functions for diurnal modes normalized to a maximum value of unity Normalization factors are 0.038, 0.130, 0.110, 0.024, and 0.018, respectively

Vertical wavelengths of some tidal modes
Isothermal Atmosphere: T=250 K

Diurnal (km)
Migrating

Mode	(1,-2)	(1,-4)	(1,1)	(1,3)	(1,5)
s=1, W	evanescent	evanescent	28	11	7

Non-mograting

Mode	(1,1)	(1,2)	(1,3)	(1,4)	(1,5)
s=0	102	26	15	11	9

Mode	(1,1)	(1,2)	(1,3)	(1,4)	(1,5)
s=-1, E	external	53	24	15	11

Mode	(1,1)	(1,2)	(1,3)	(1,4)	(1,5)
s=2,W	27	16	11	9	7

Mode	(1,1)	(1,2)	(1,3)	(1,4)	(1,5)
s=-2, E	108	38	21	14	10

Mode	(1,1)	(1,2)	(1,3)	(1,4)	(1,5)
s=5, W	19	13	10	8	7

Mode	(1,1)	(1,2)	(1,3)	(1,4)	(1,5)
s=-5, E	31	21	15	12	9

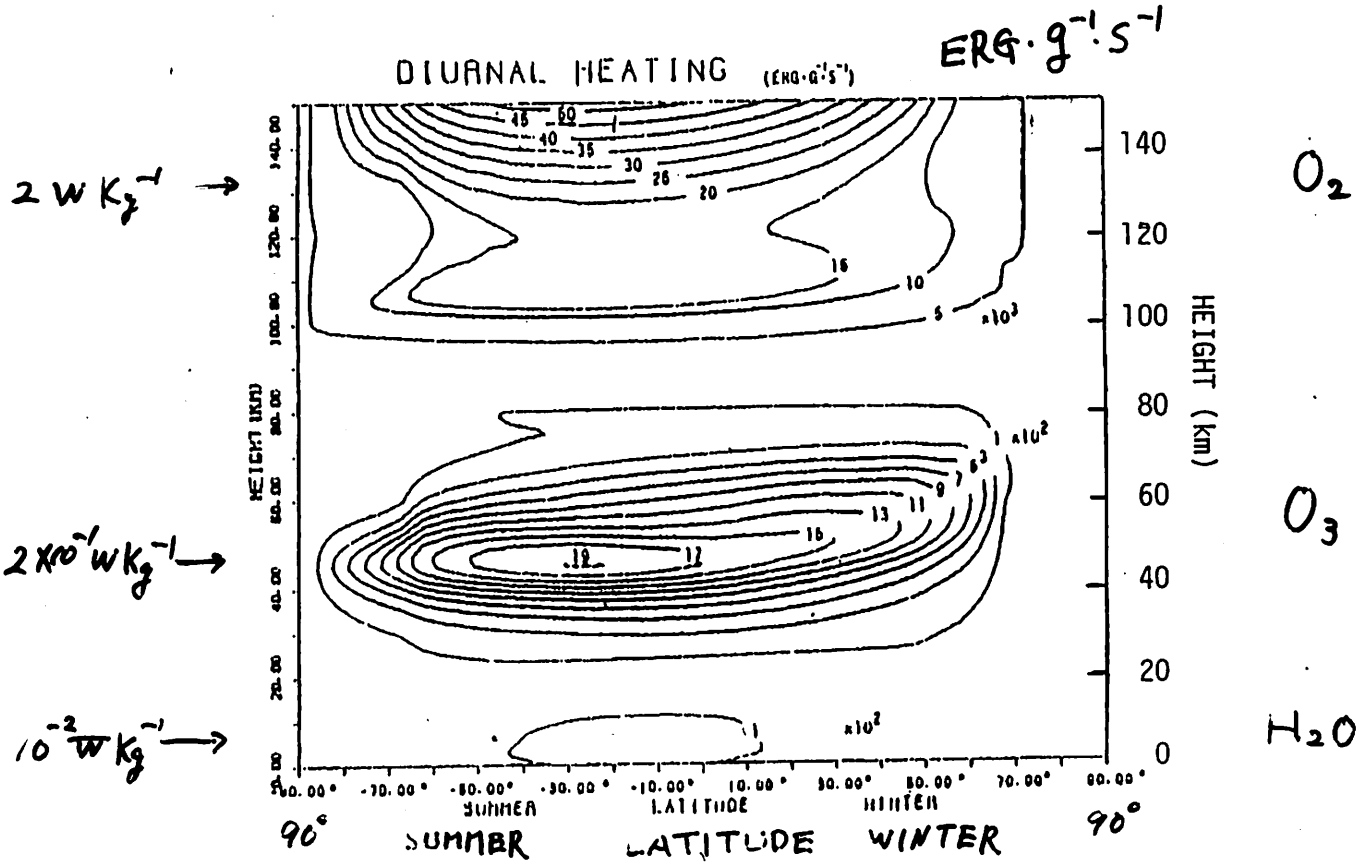

Fig.1 Meridional cross section of tide-generating heating for solstice.

Miyahara (1984)

UARS (WINDII + HRDI)

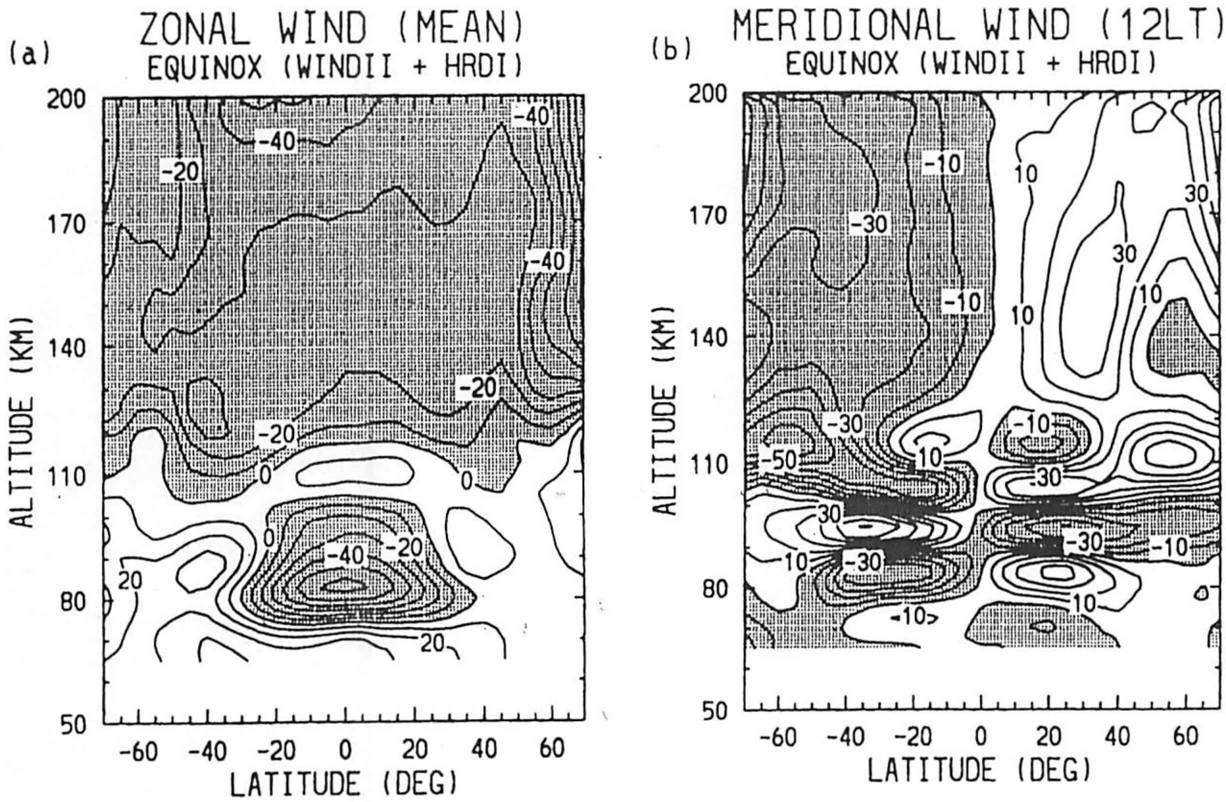

Feb. 12 to May 3, 1993

McLandress et al. (1996)

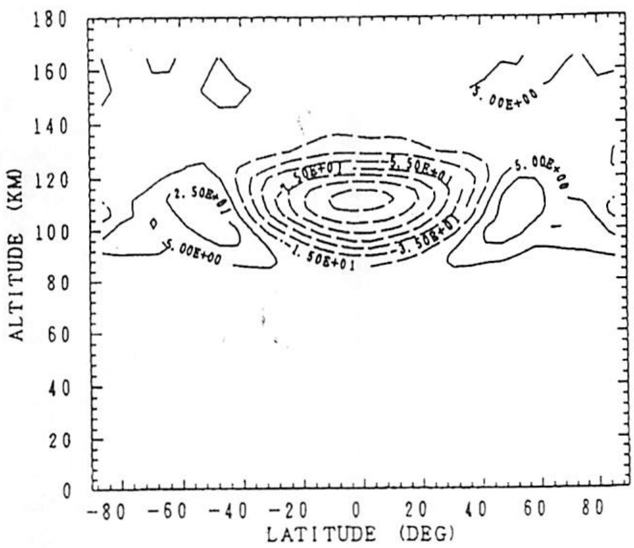

Fig. 16. Meridional cross section of the induced mean zonal winds. Dashed lines denote easterlies. The contour interval is 20 ms^{-1}.

Wu et al. (1993)

Numerical simulation (non-linear)

Hagan et al. (1997) UARS - WINDII

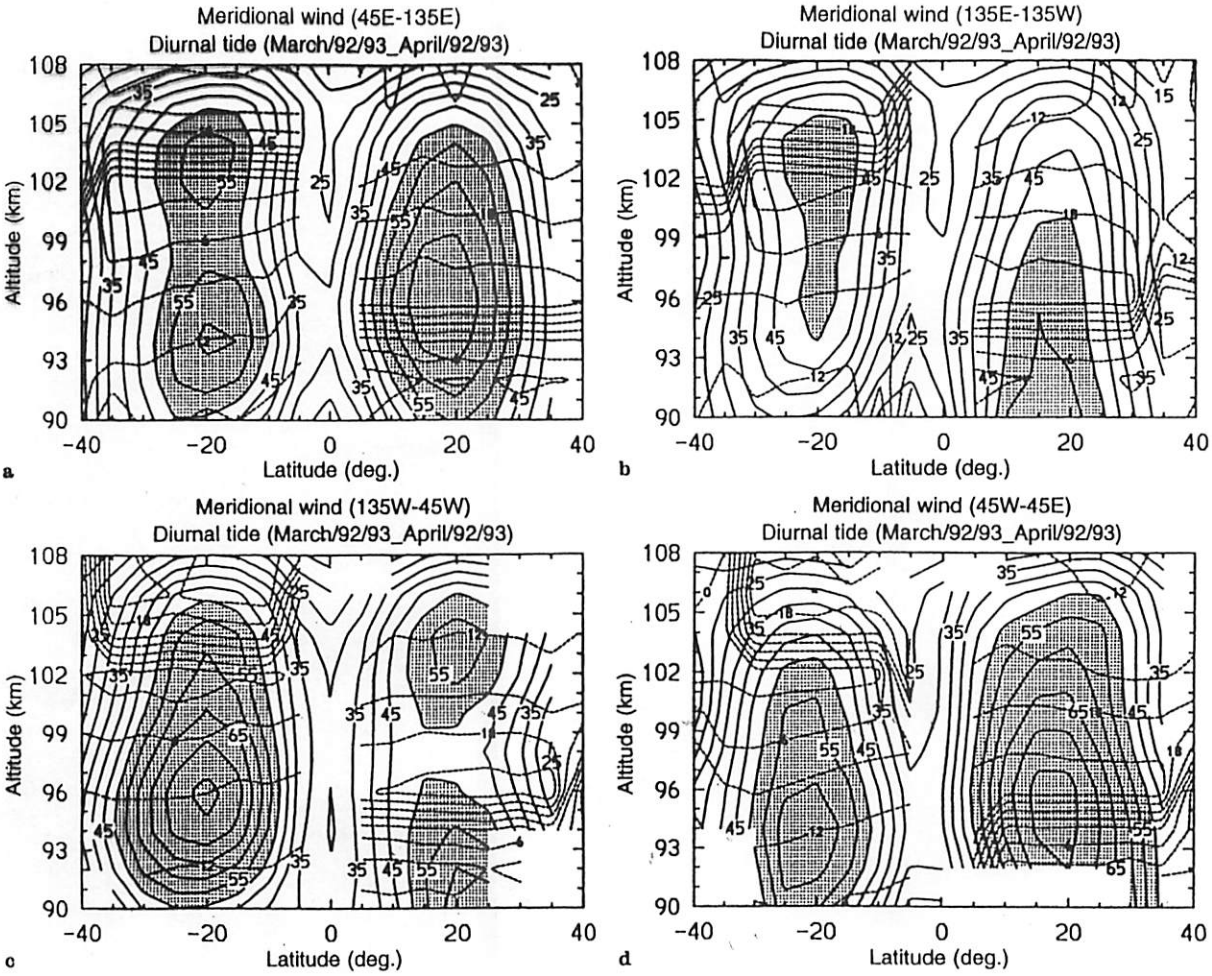

Fig. 1. Contours of meridional wind amplitude (*solid lines*) and phase (*dashed lines*) of the diurnal tide observed by WINDII for March/April 1992 and 1993 at **a** 45°E to 135°E, **b** 135°E to 135°W, **c** 135°W to 45°W, and **d** 45°W to 45°E longitude sectors. Amplitude contours >50 m/s are shaded. The phase (local time of maximum) is contoured using a 3-h interval

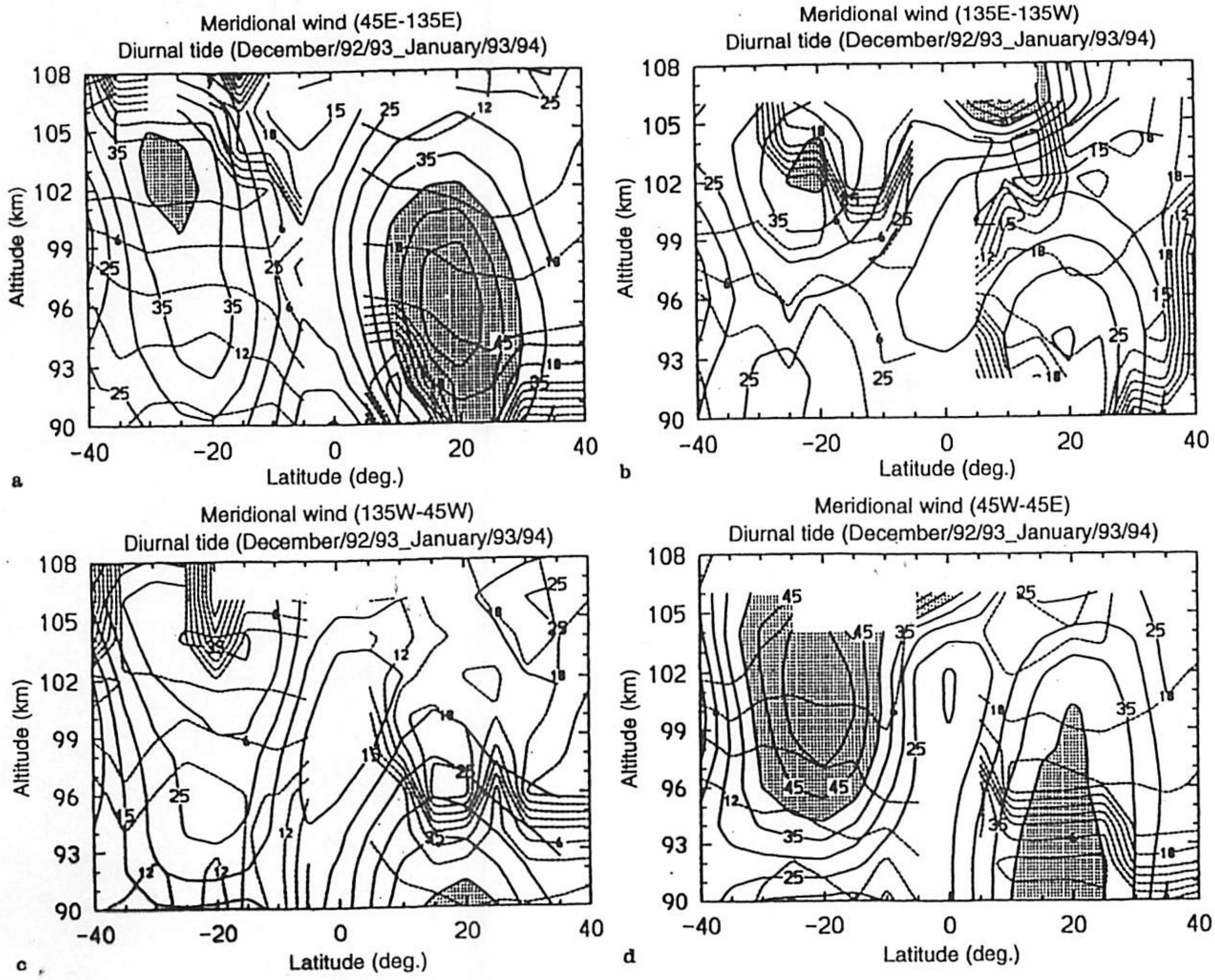

Fig. 2a–d. Contours of meridional wind amplitude (*solid lines*) and phase (*dashed lines*) of the diurnal tide observed by WINDII for December 1992, 1993 and January 1993, 1994 at: **a** 45°E to 135°E, **b** 135°E to 135°W, **c** 135°W to 45°W, and **d** 45°W to 45°E longitude sectors. Amplitude contours >40 m/s are shaded. The phase (local time of maximum) is contoured using a 3-h interval

16

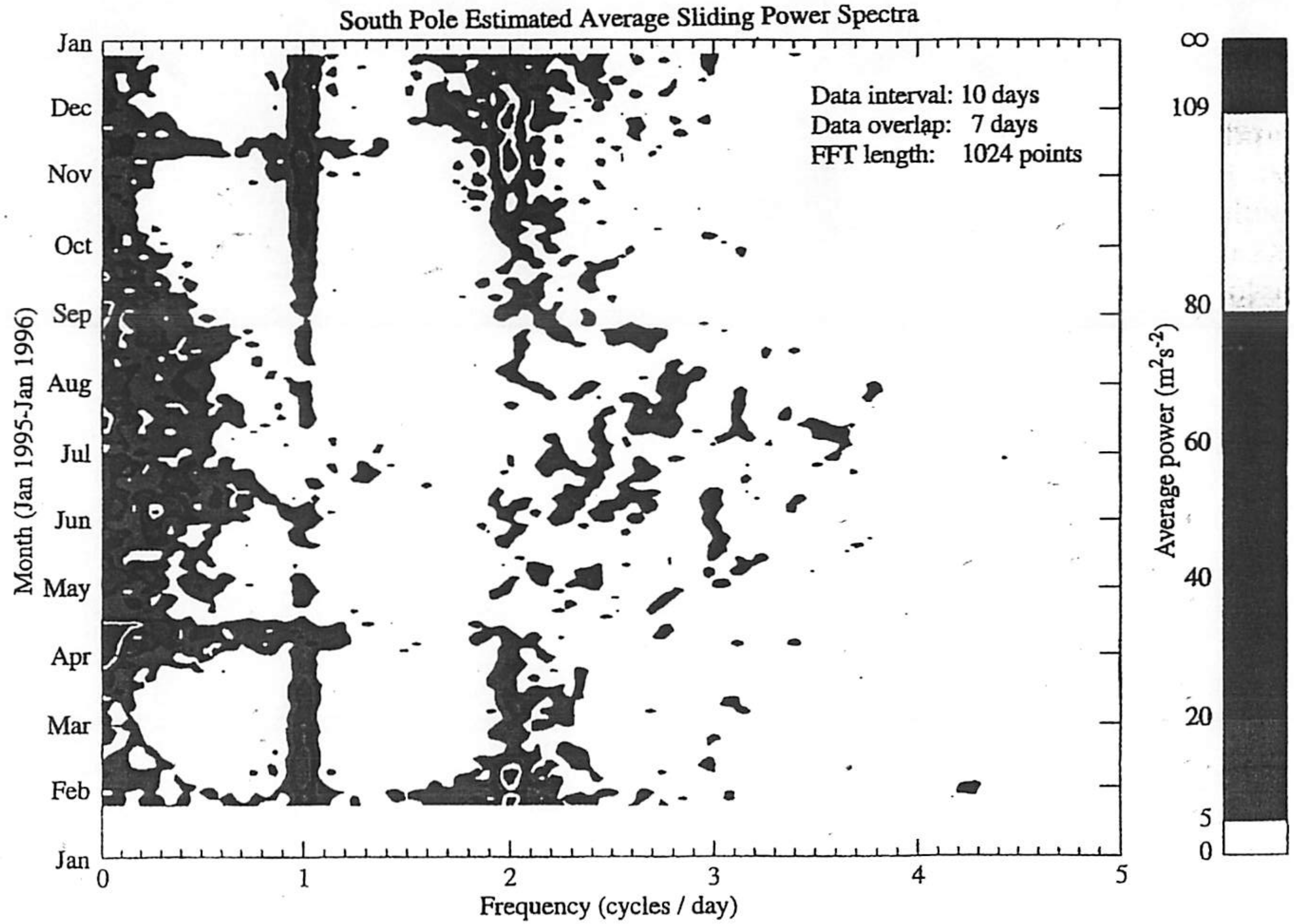

Fig. 1. Average spectrogram of the hourly meridional winds over the four directions of measurement. The spectrogram is formed by sliding 10-day spectra in increments of 3 days from 19 January 1995 to 26 January 1996

Forbes et.al. 1995
Portnyagin et al. 1998

↑
, westward propagating
S=1
NON-MIGRATING

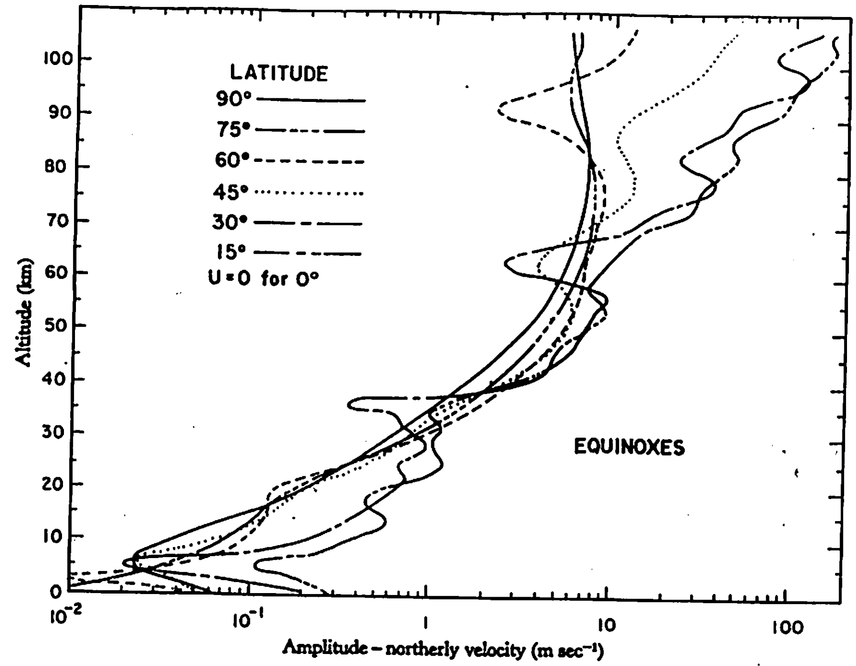

Fig. 3.13. Altitude distribution of the amplitude of the solar diurnal component of *u* at 15° intervals of latitude; isothermal basic state assumed. After Lindzen (1967a).

Wu, Miyahara, and Miyoshi (1985)

A nonlinear simulation of the thermal diurnal tide

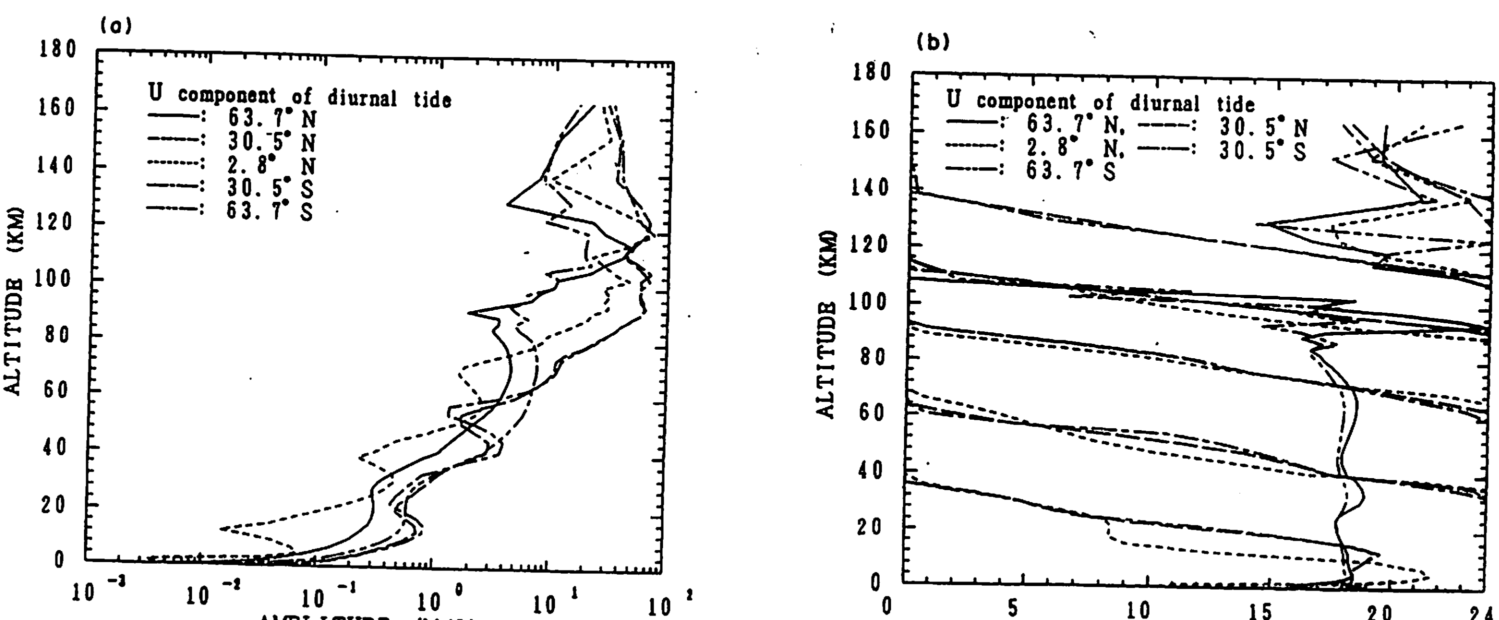

Fig. 4. Vertical profiles of (a) amplitudes and (b) phases, of zonal velocities of the diurnal tide at various latitudes.

Diurnal Temperature

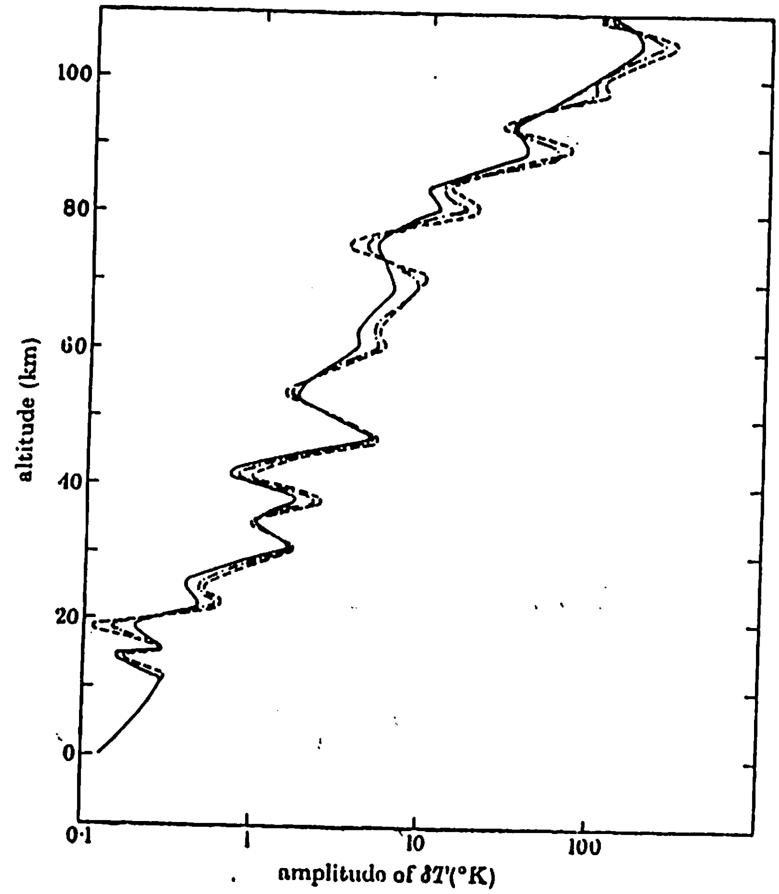

FIGURE 3. Amplitude of the diurnal temperature oscillation over the equator for different distributions of the cooling rate coefficient: ——, standard; —·—, without photochemical acceleration; – – – –, zero.

Ri.

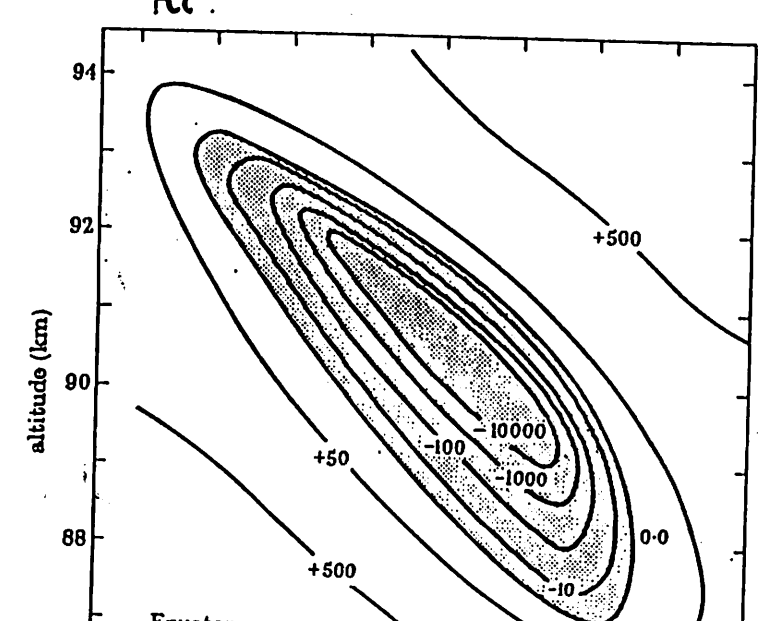

FIGURE 7. Time-height cross-section of the Richardson number over the equator.

Lindzen (1968)

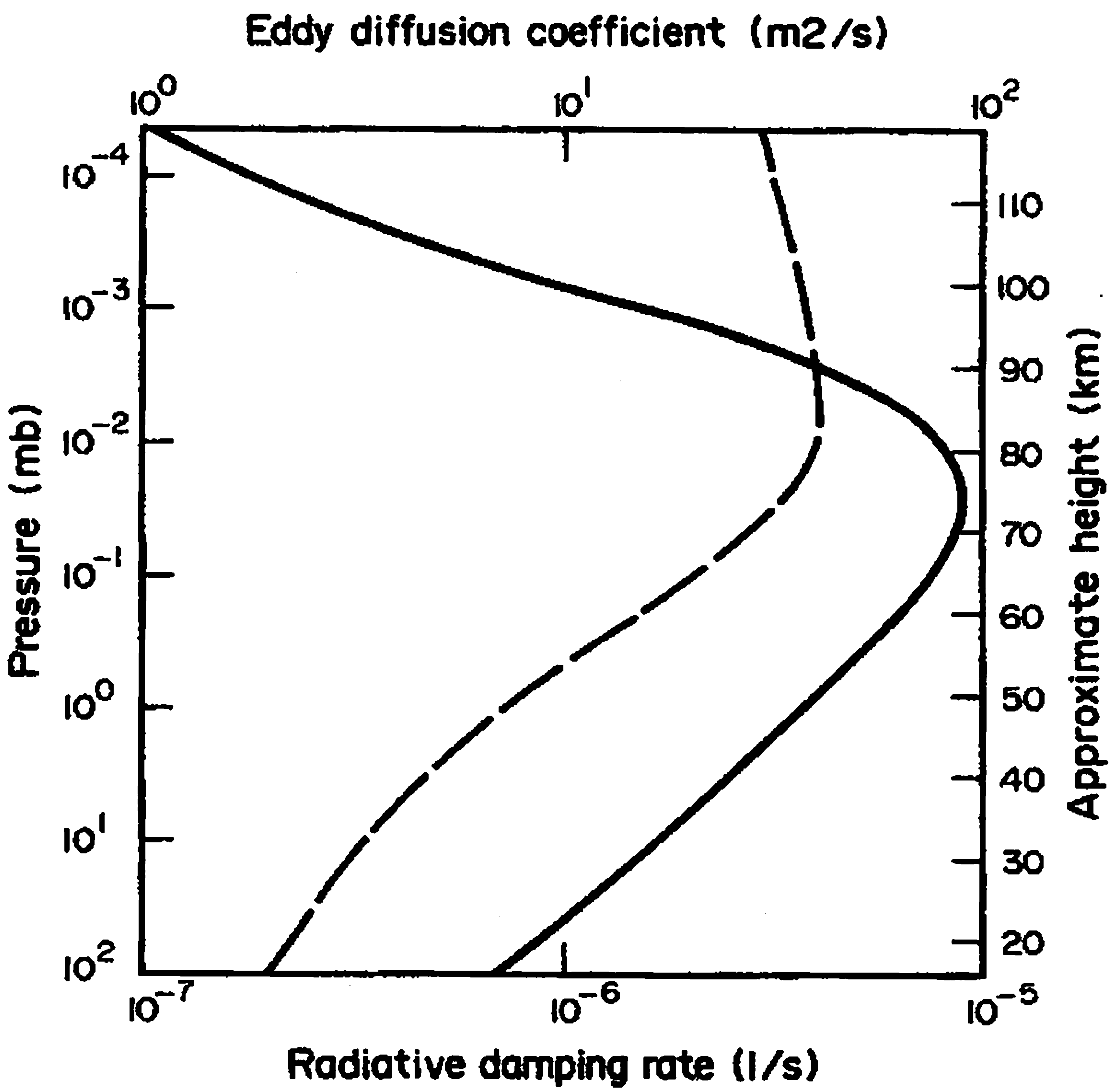

Fig. 1. The radiative damping rate (solid) and the vertical eddy diffusion coefficient (dashed).

Akmaev et al. (1992)

Monthly mean amplitudes of diurnal tides (UARS - HRDI)

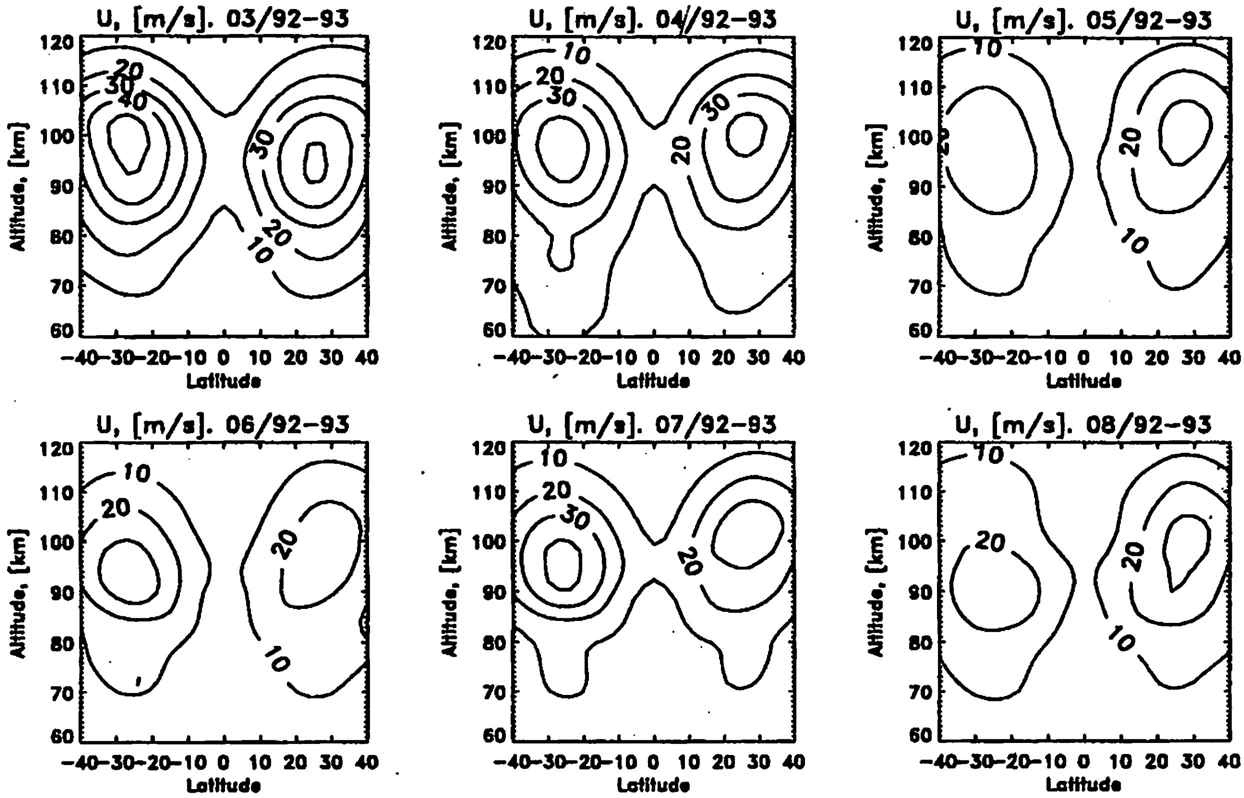

Vertical eddy diffusion coefficients derived from HRDI data

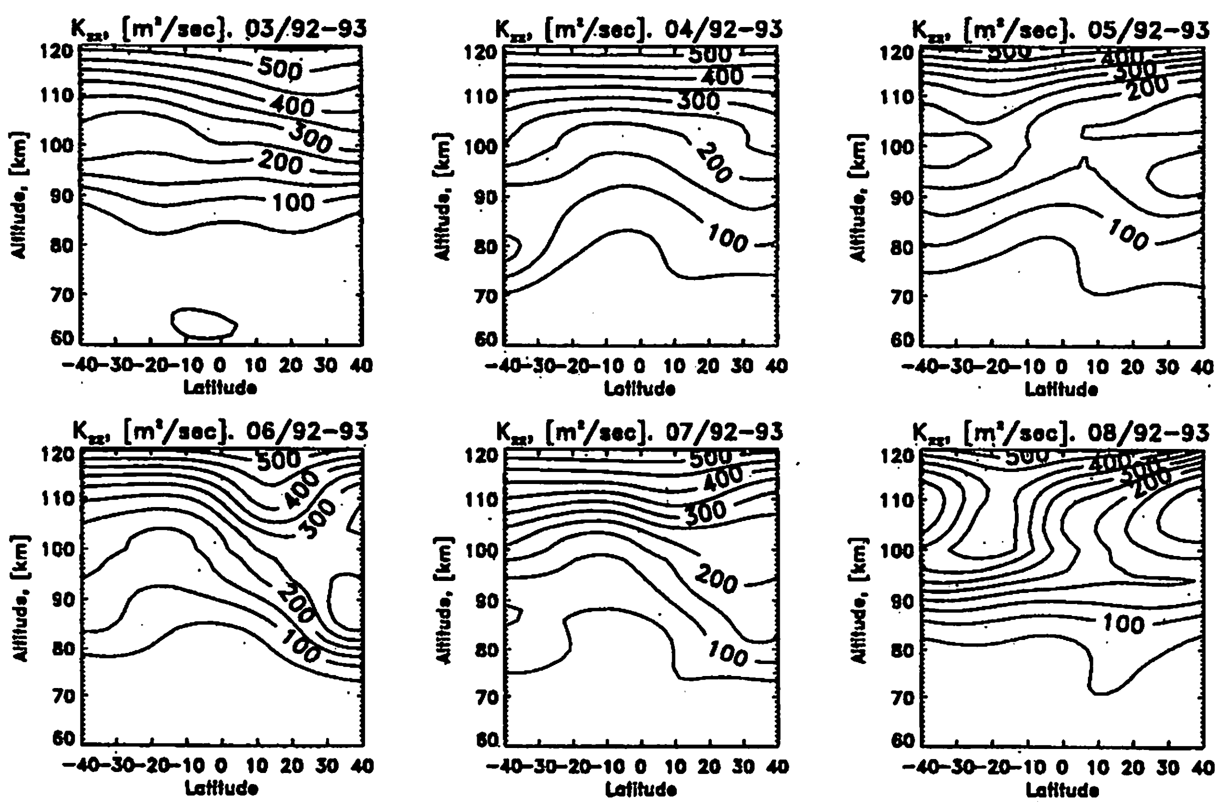

Khattatov et al., (1997)

Middle Atmosphere Circulation Model at Kyushu University MACMKU

- T21L55, General Circulation Model (GCM)
- Height Range: Ground through about 150 km
- Solar Radiation: having diurnal cycle,

  H_2O, O_3, and O_2 heating,

  H_2O: Predicted in the model

  (Troposphere: non-zonal)

  O_3, and O_2: zonally symmetric distribution
- Infrared radiation: Fomichev's parameterization

  Troposphere: Chou's parameterization
- Land Temperature: Predicted in the model
- SST: Prescribed monthly mean SST
- Tropospheric physical processes

  Latent heat, Topography, etc.
- Dissipation processes in the MLT

  Molecular viscosity and conductivity

  Ion drag (Local time dependent)

  Dry convective adjustment

  Eddy diffusion

  Rayleigh Friction (Only for the zonal mean zonal winds in the MLT)

  No gravity wave drag parameterization

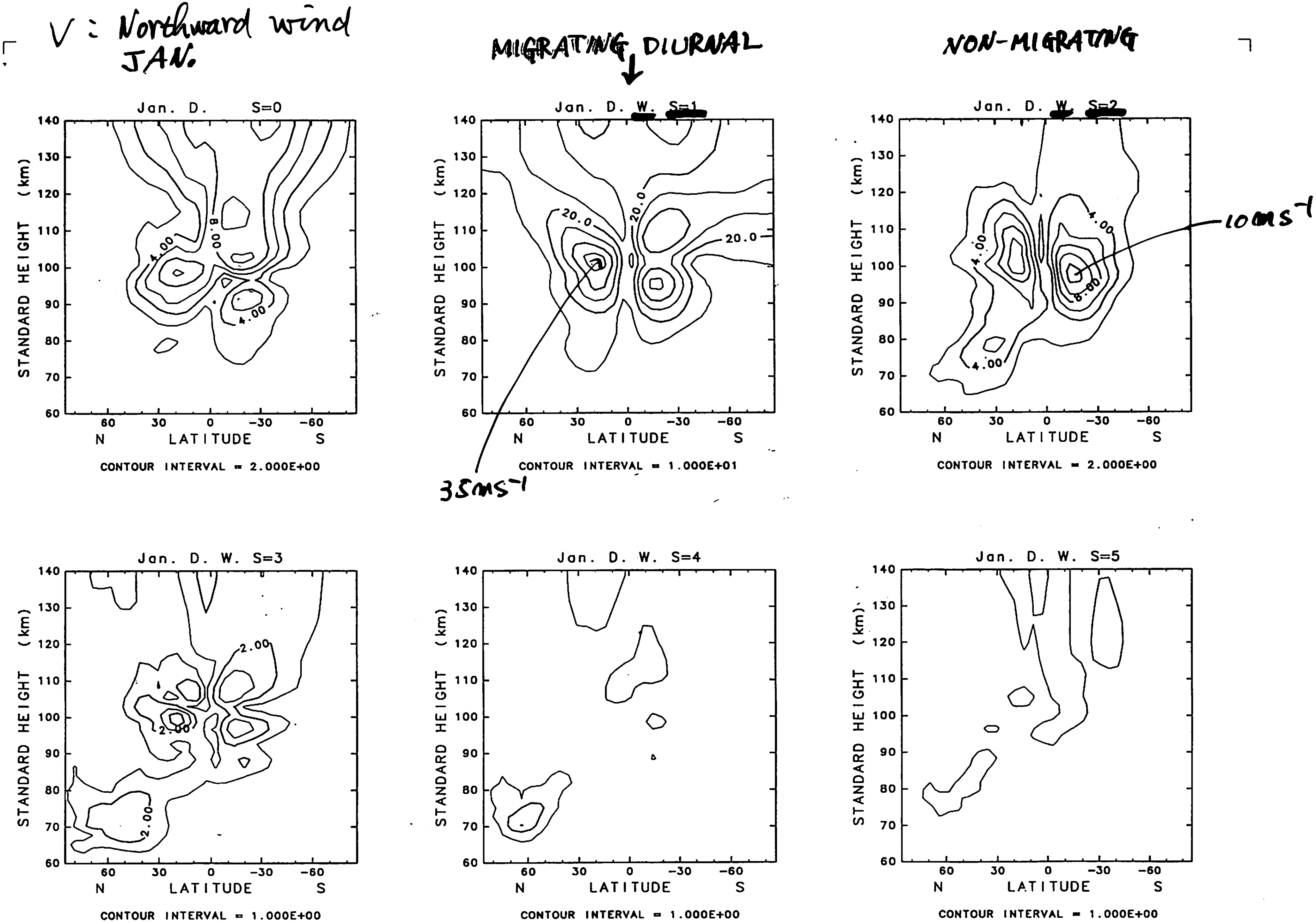
V : Northward wind
JAN.
MIGRATING DIURNAL
NON-MIGRATING
Jan. D. S=0
Jan. D. W. S=1
Jan. D. W. S=2
Jan. D. W. S=3
Jan. D. W. S=4
Jan. D. W. S=5
STANDARD HEIGHT (km)
LATITUDE
N
S
CONTOUR INTERVAL = 2.000E+00
CONTOUR INTERVAL = 1.000E+01
CONTOUR INTERVAL = 2.000E+00
CONTOUR INTERVAL = 1.000E+00
CONTOUR INTERVAL = 1.000E+00
CONTOUR INTERVAL = 1.000E+00
35ms-1
10ms-1

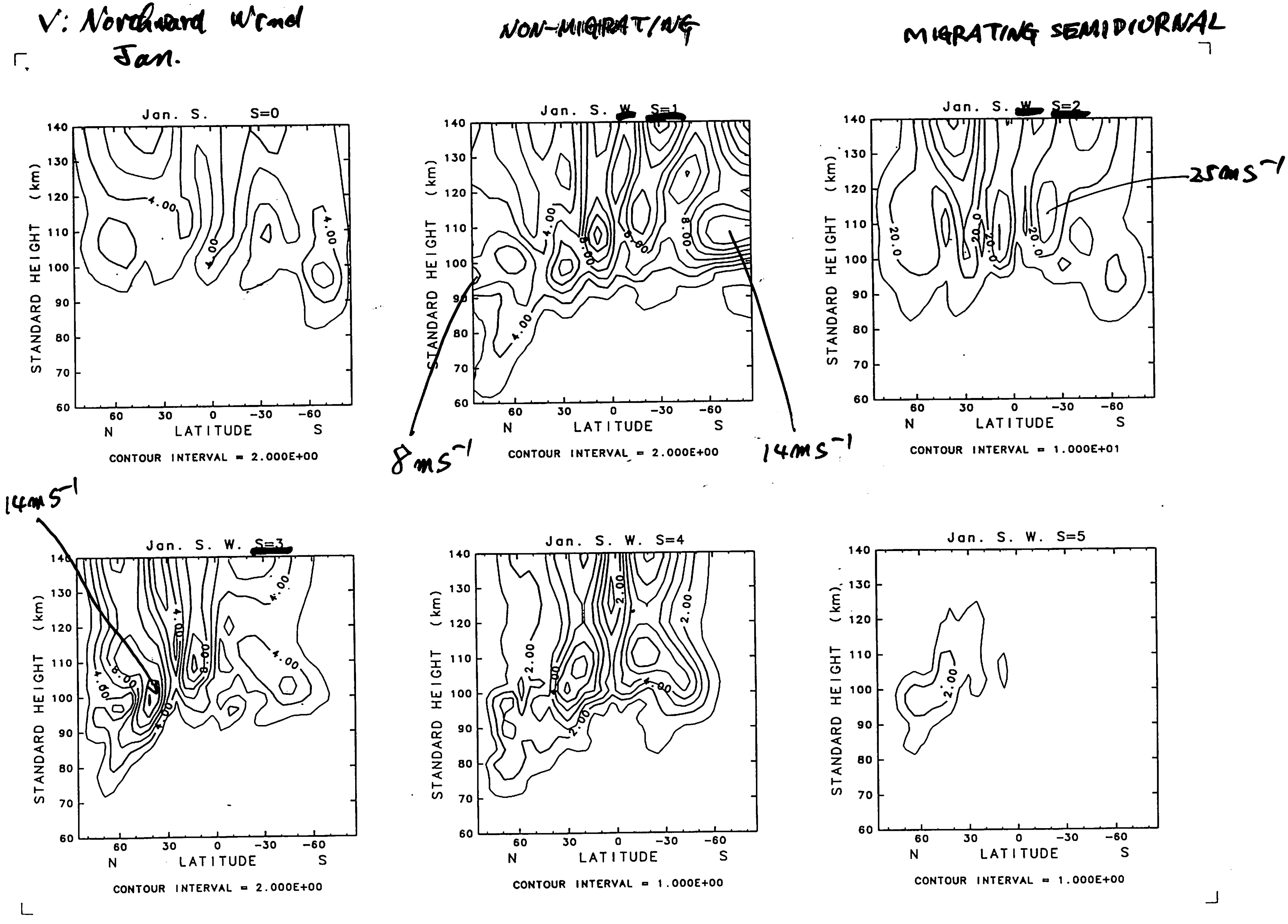
V: Northward Wind
Jan.
NON-MIGRATING
MIGRATING SEMIDIURNAL
Jan. S. S=0
STANDARD HEIGHT (km)
LATITUDE
N
S
CONTOUR INTERVAL = 2.000E+00
Jan. S. W. S=1
8 ms⁻¹
14 ms⁻¹
CONTOUR INTERVAL = 2.000E+00
Jan. S. W. S=2
25 ms⁻¹
CONTOUR INTERVAL = 1.000E+01
14 ms⁻¹
Jan. S. W. S=3
CONTOUR INTERVAL = 2.000E+00
Jan. S. W. S=4
CONTOUR INTERVAL = 1.000E+00
Jan. S. W. S=5
CONTOUR INTERVAL = 1.000E+00

Ebanayake Dr. Thesis

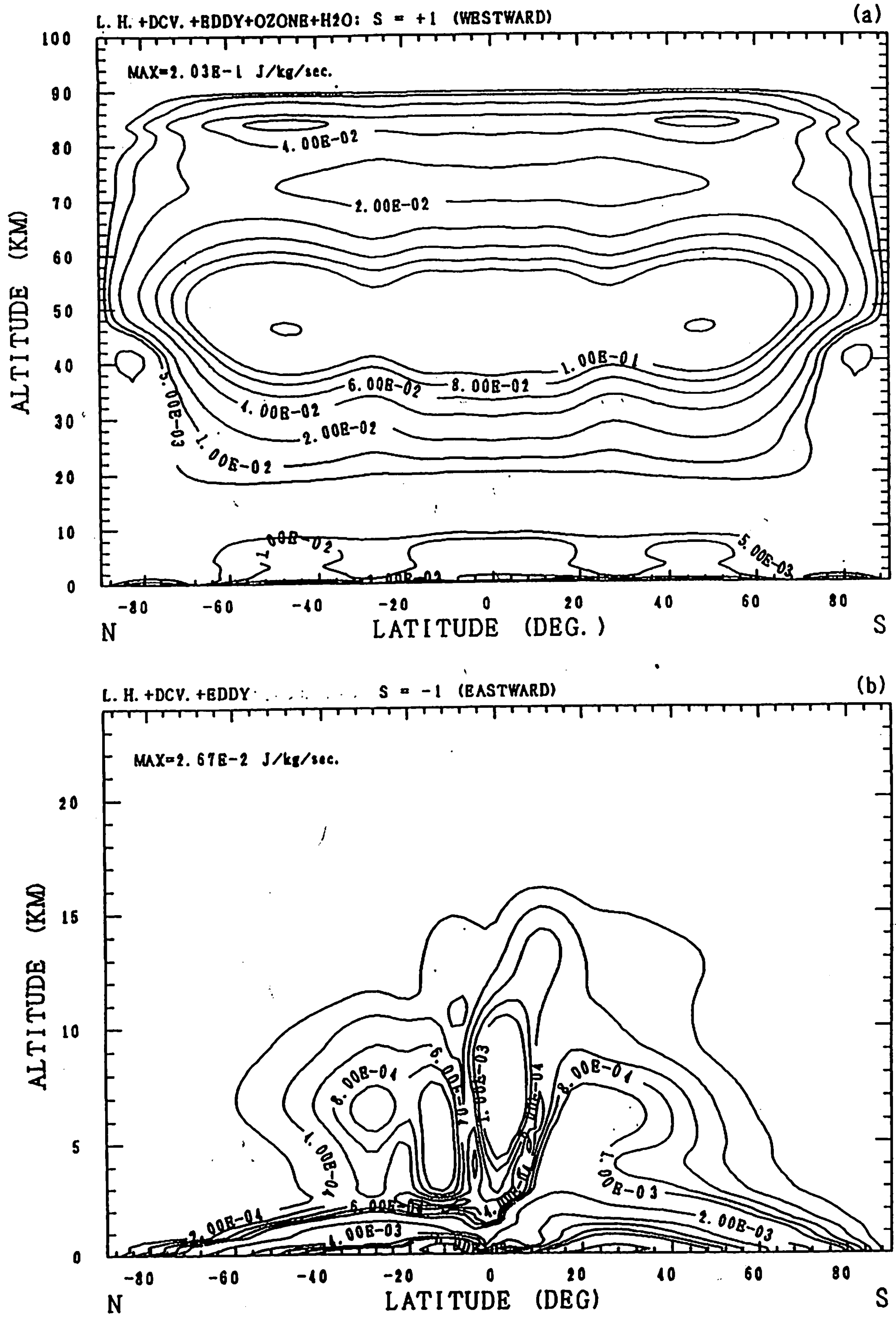

Fig.(4.1.2) Latitude dependence of total forcing which includes latent heating, heating due to dry convection, eddy thermal conduction and insolation absorption by water vapor in the troposphere and ozone absorption heating in the middle atmosphere for s = +1, (a), and s = -1, (b).

25

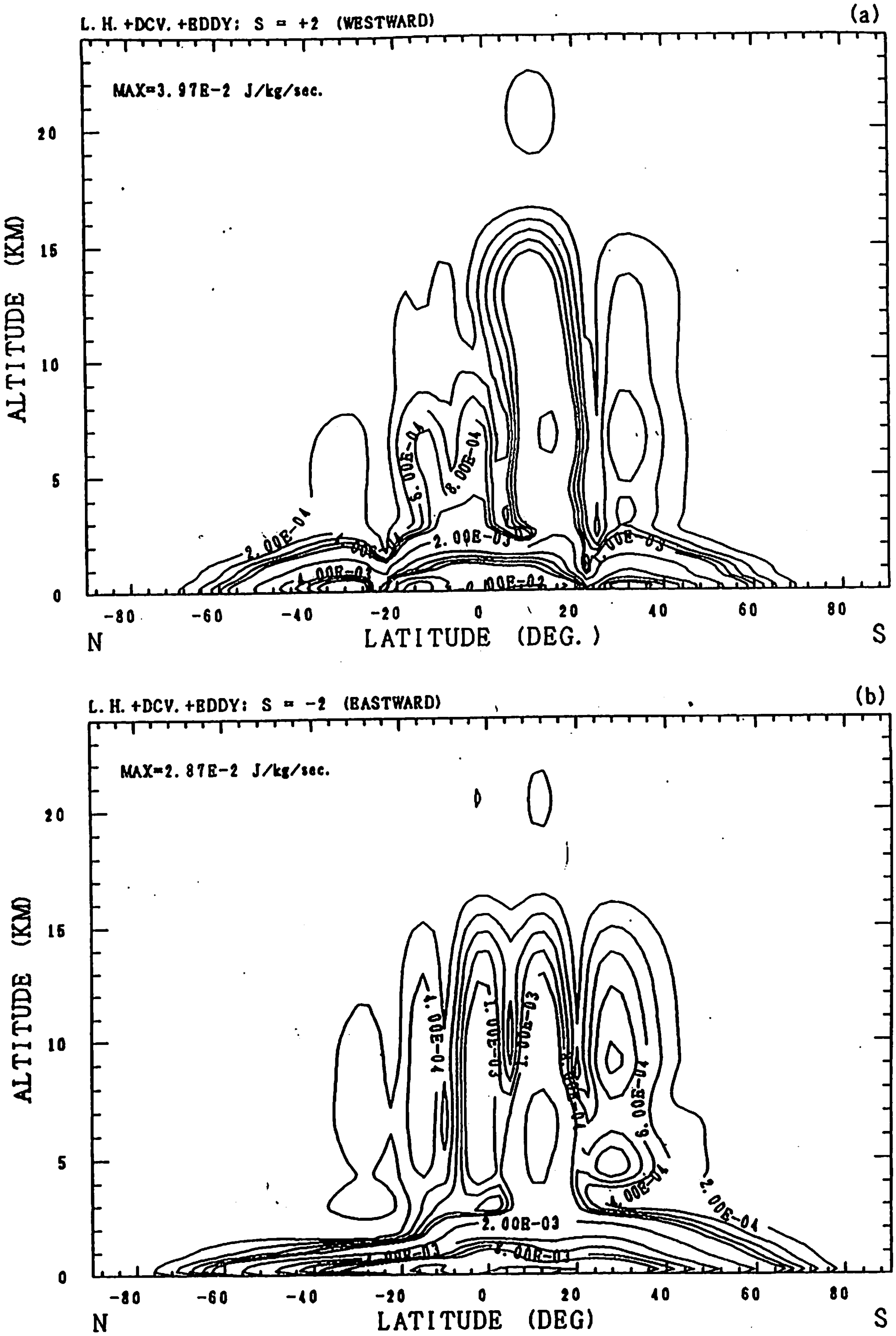

Fig.(4.1.3) As in Fig.(4.1.1) except for s = +2, (a), and s = -2, (b).

Linear model result by the GCM heating.

(Ekanayake et al. 1997)

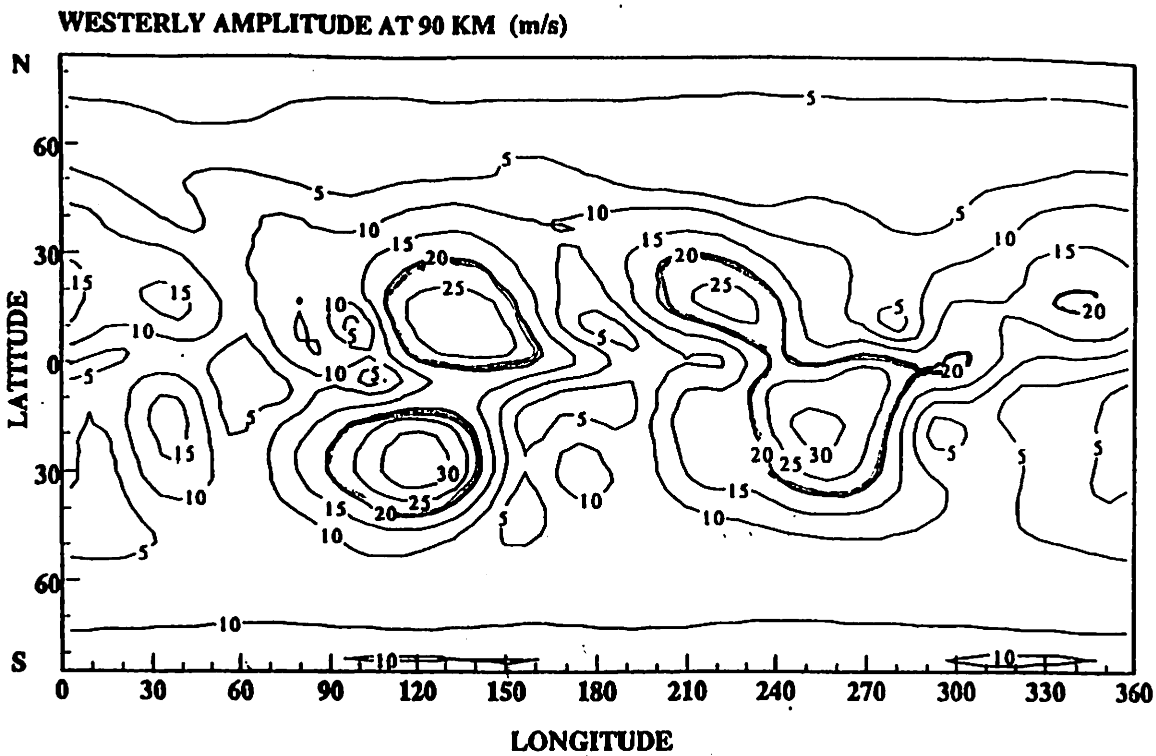

—20ms⁻

GCM result

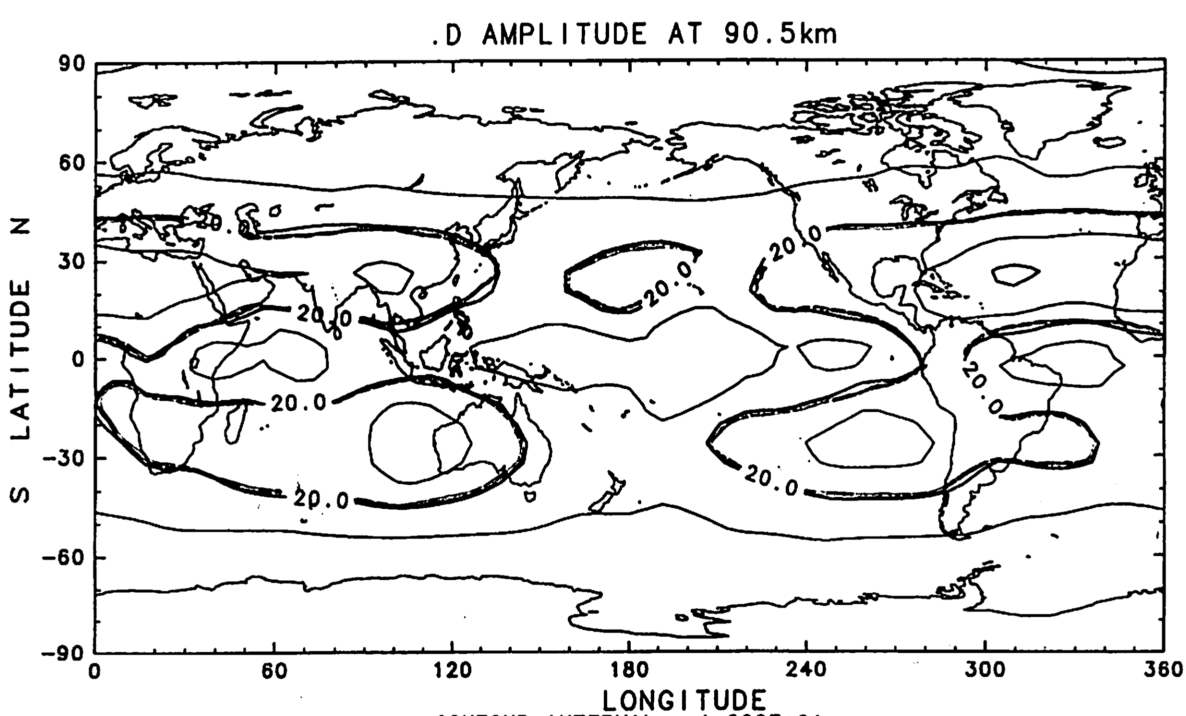

—20ms⁻¹

GCM (MACMKU)

AMPLITUDE V

January S.W. S=1

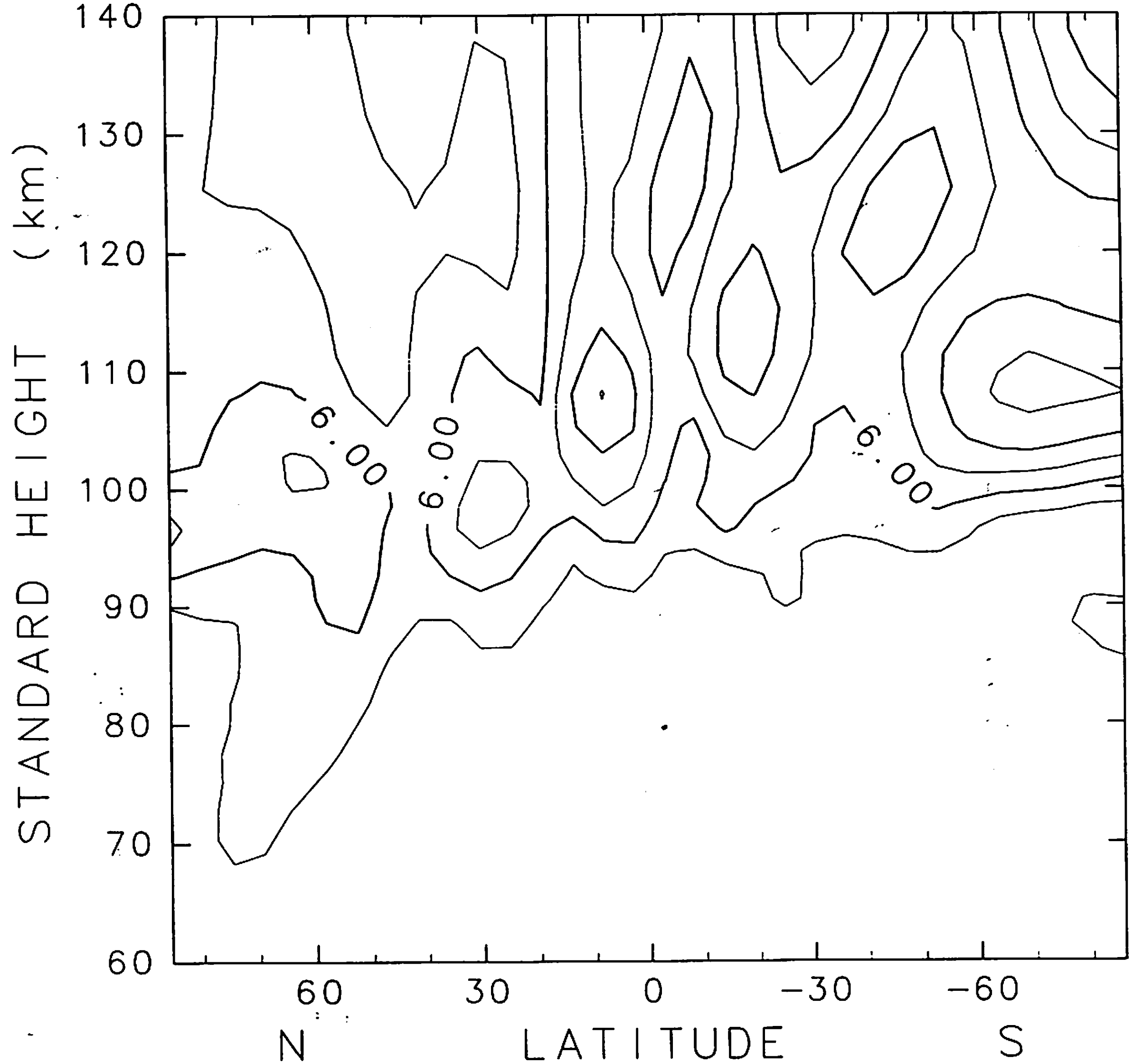

CONTOUR INTERVAL = 3.000E+00

Fig. 1a

number s=1 becomes large in the summer season at the north and south polar MLT regions. Two different possible excitation mechanisms of the non-migrating semidiurnal tide are suggested (Forbes et al., 1995; Portnyagin et al., 1998). One is non-migrating heating in the troposphere associated with latent heat release. The other is nonlinear interaction between the migrating semidiurnal tide and a stationary planetary wave with zonal wavenumber s=1. In this section the later mechanism is investigated using the output data of the MACMKU.

3-1. Source of excitation

The idea of the nonlinear interaction forcing is as follows. The nonlinear interaction terms in the governing equation system expressed by the pressure coordinate system in the MACMKU are given by the advection terms. The nonlinear forcing terms due to a planetary wave and the semidiurnal tide are given by

$$F_\lambda = \frac{u_{pl}}{a\cos\theta}\frac{\partial u_{sd}}{\partial\lambda} + \frac{v_{pl}}{a\cos\theta}\frac{\partial}{\partial\theta}\left(u_{sd}\cos\theta\right) + \omega_{pl}\frac{\partial u_{sd}}{\partial p}$$

$$+\frac{u_{sd}}{a\cos\theta}\frac{\partial u_{pl}}{\partial\lambda} + \frac{v_{sd}}{a\cos\theta}\frac{\partial}{\partial\theta}\left(u_{pl}\cos\theta\right) + \omega_{sd}\frac{\partial u_{pl}}{\partial p}, \qquad (3.1)$$

$$F_\theta = \frac{u_{pl}}{a\cos\theta}\frac{\partial v_{sd}}{\partial\lambda} + \frac{v_{pl}}{a}\frac{\partial v_{sd}}{\partial\theta} + \omega_{pl}\frac{\partial v_{sd}}{\partial p}$$

$$+\frac{u_{sd}}{a\cos\theta}\frac{\partial v_{pl}}{\partial\lambda} + \frac{v_{sd}}{a}\frac{\partial v_{pl}}{\partial\theta} + \omega_{sd}\frac{\partial v_{pl}}{\partial p} + (2u_{sd}u_{pl})\frac{\tan\theta}{a}, \qquad (3.2)$$

$$F_T = \frac{u_{pl}}{a\cos\theta}\frac{\partial T_{sd}}{\partial\lambda} + \frac{v_{pl}}{a}\frac{\partial T_{sd}}{\partial\theta} + \omega_{pl}\left(\frac{\partial T_{sd}}{\partial p} - \frac{R}{c_p p}T_{sd}\right)$$

$$+\frac{u_{sd}}{a\cos\theta}\frac{\partial T_{pl}}{\partial\lambda} + \frac{v_{sd}}{a}\frac{\partial T_{pl}}{\partial\theta} + \omega_{sd}\left(\frac{\partial T_{pl}}{\partial p} - \frac{R}{c_p p}T_{pl}\right), \qquad (3.3)$$

Semi diurnal forcing with s=1 and s=3
(Westward moving)

AMPLITUDE

Result of a linear response model with $\bar{u}$ of GCM.

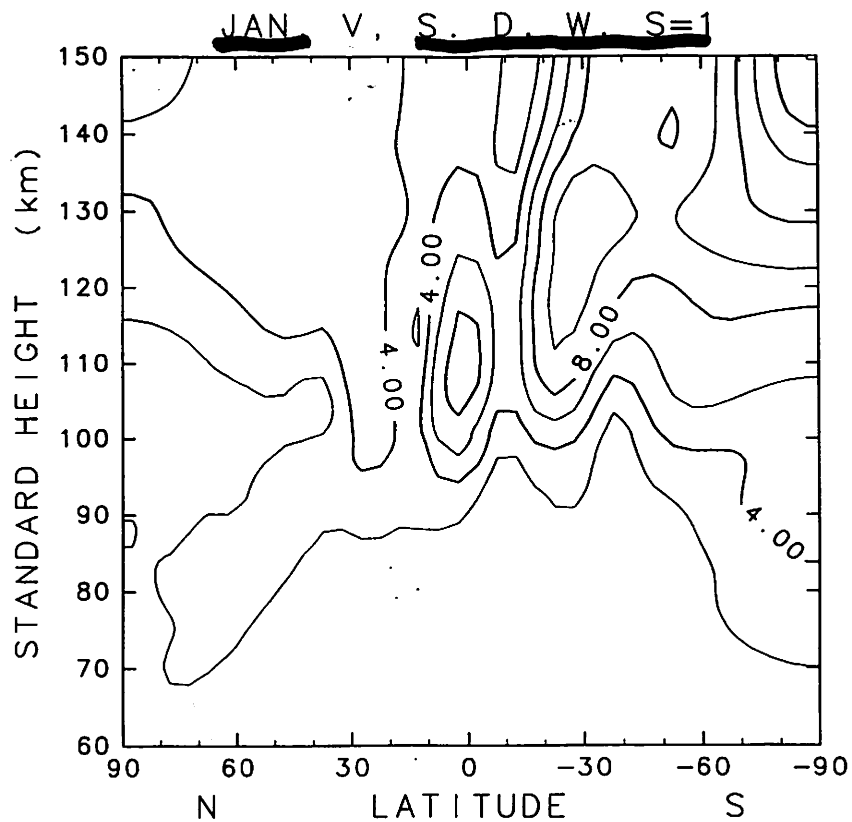

CONTOUR INTERVAL = 2.000E+00

Fig. 8a

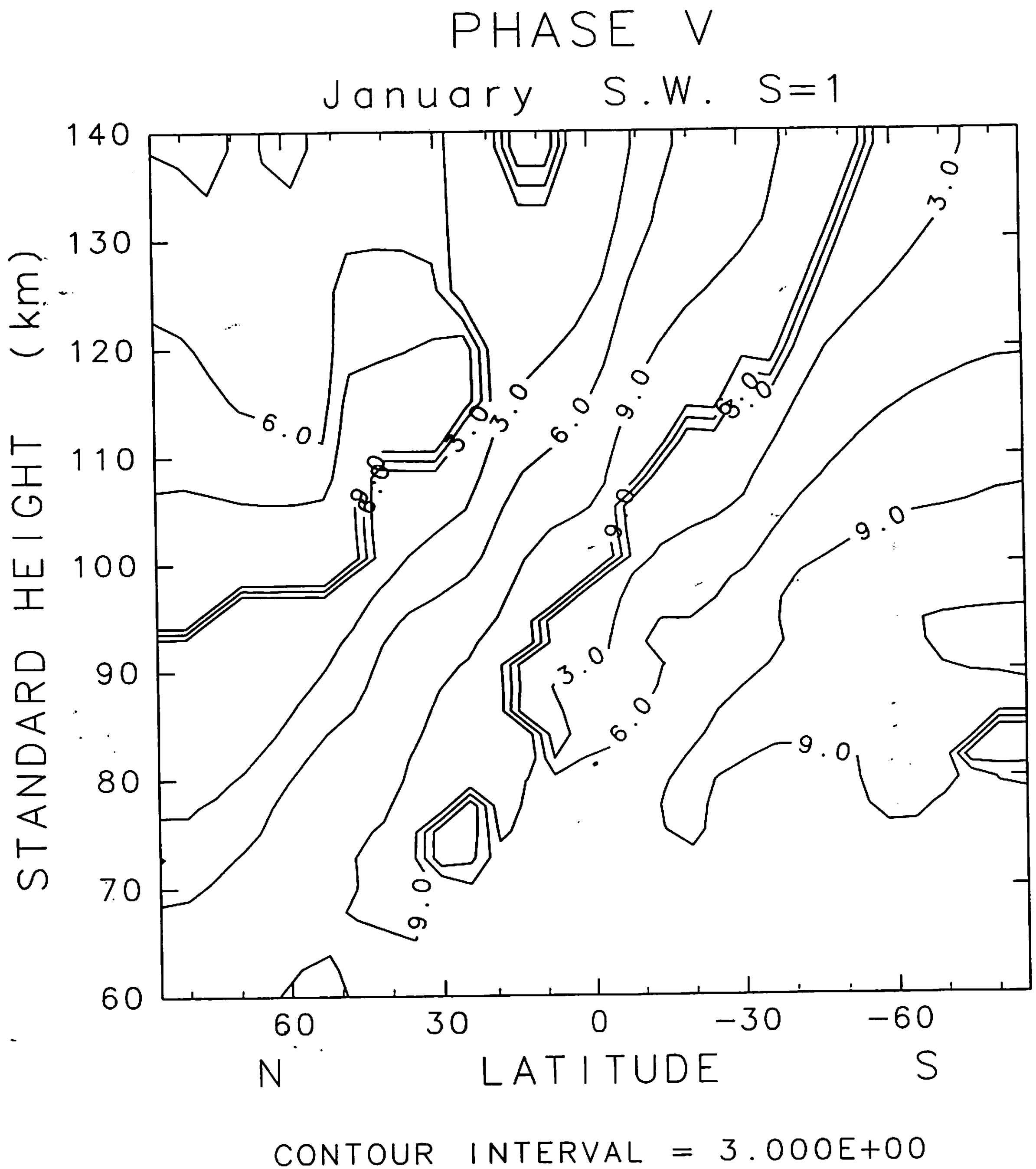

GCM
(MACMKU)

Fig. 1b

PHASE

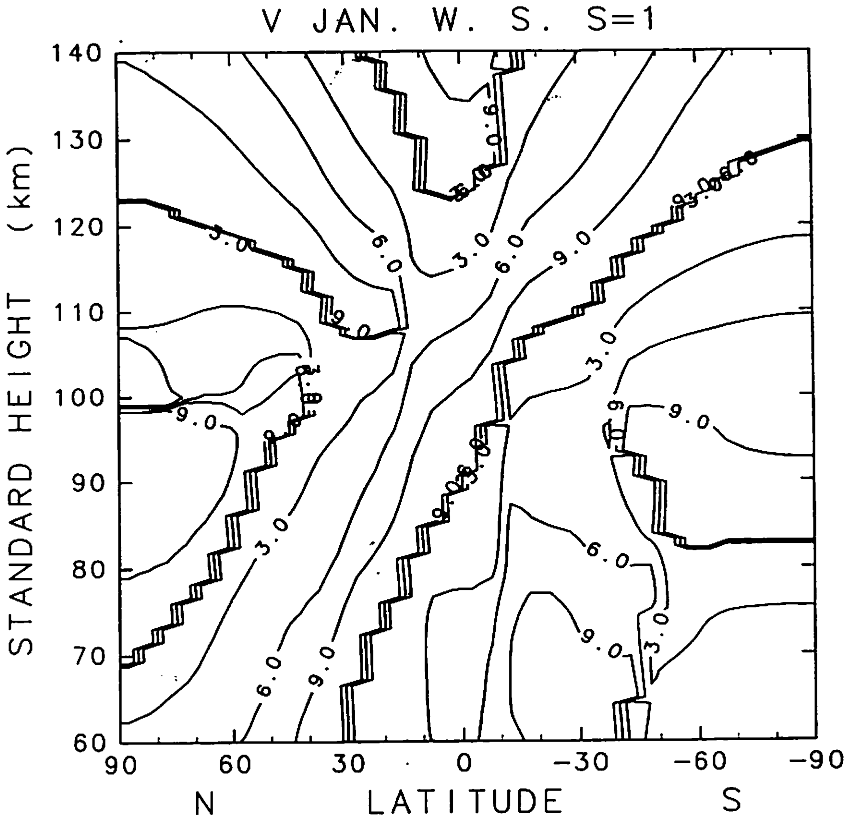

CONTOUR INTERVAL = 3.000E+00

Fig. 8b

線形応答モデル
Linear response model

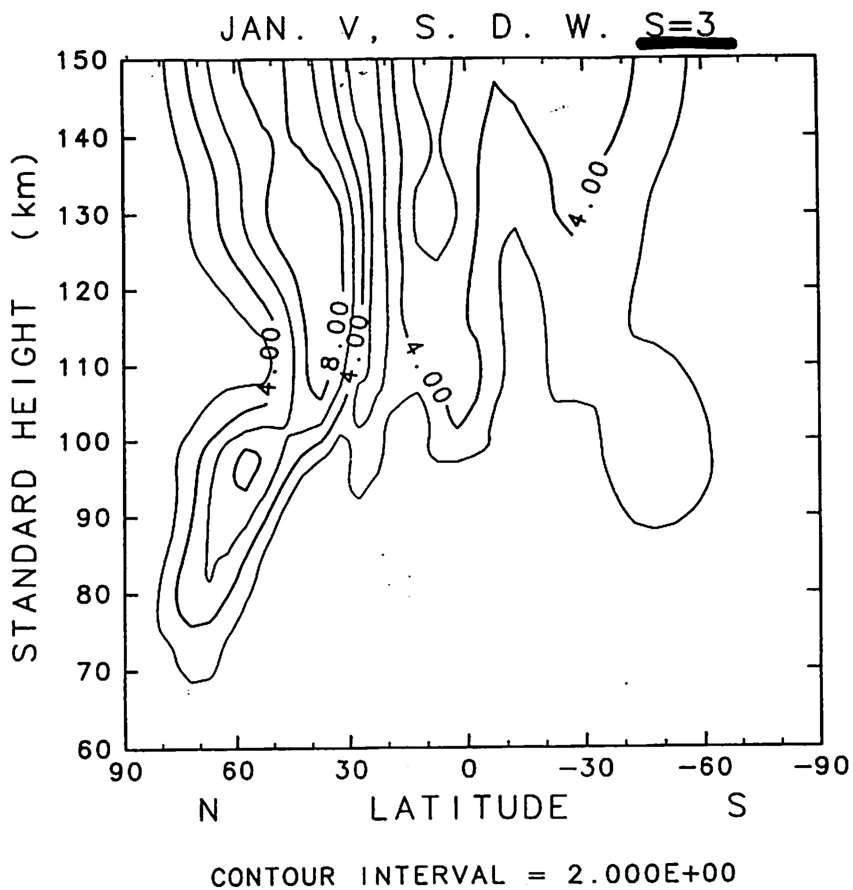

GCM (MACMKU)

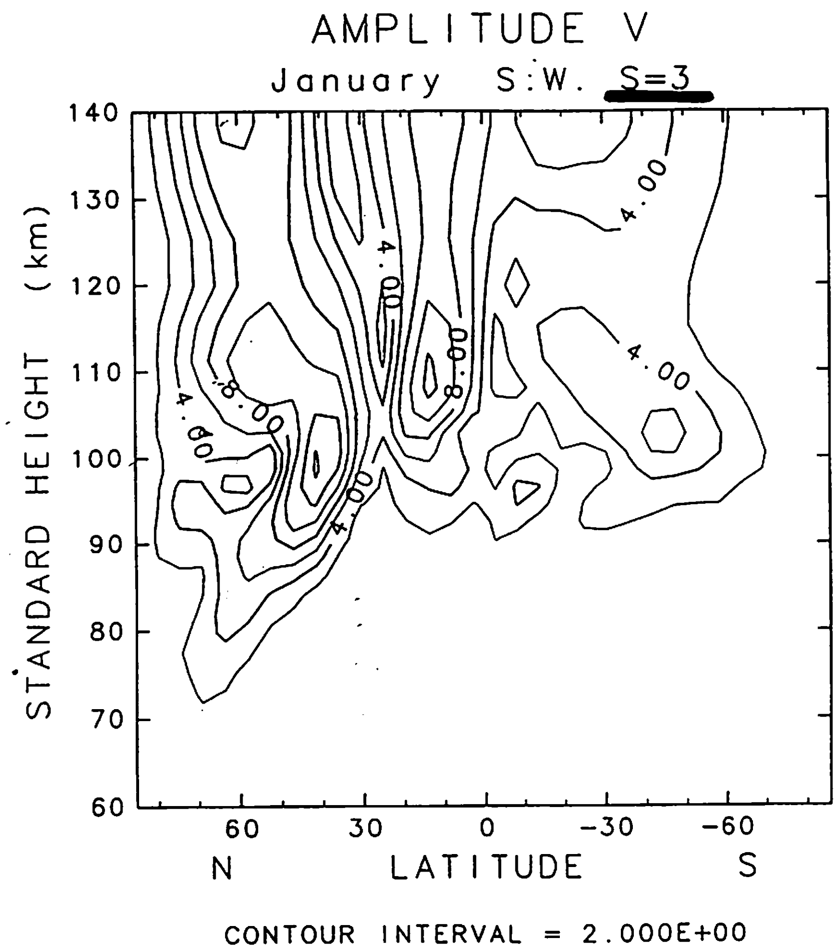

Fig. 12a

Effects of background mean zonal winds

$\overline{u}(\theta, z)$:mean zonal winds

Doppler shift of tidal frequency ω

$$\frac{\partial}{\partial t} + \frac{\overline{u}}{a\cos\theta}\frac{\partial}{\partial\lambda} = i(\omega + s\overline{u})$$

S : zonal wave number

θ: Latitude

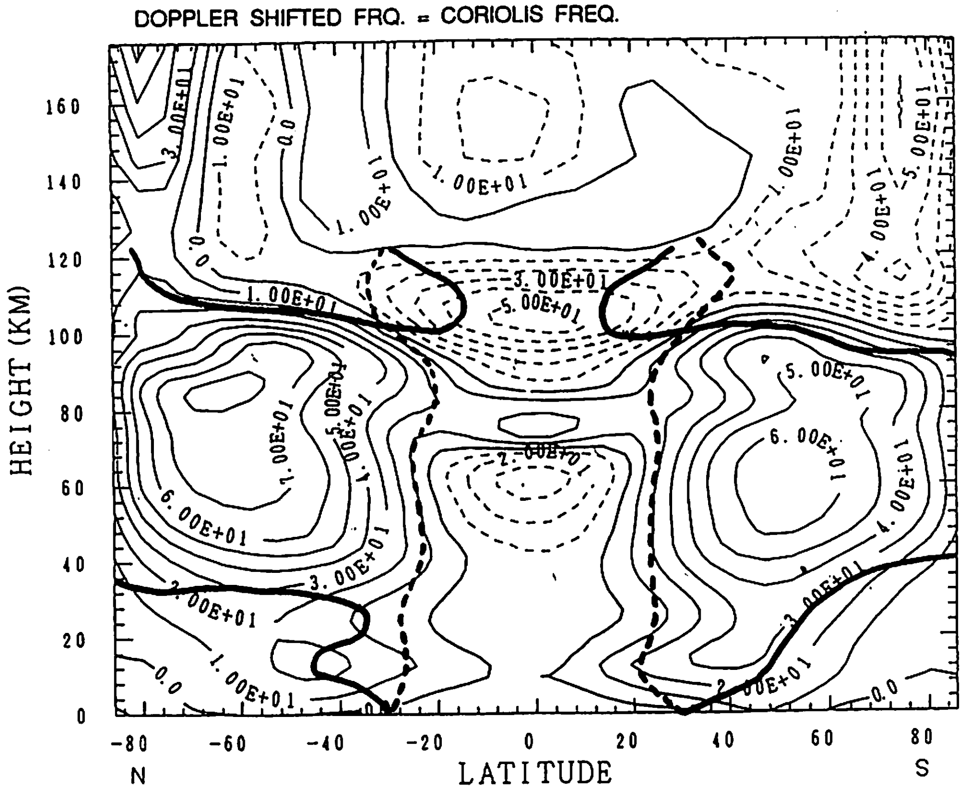

Fig. 12. Location where Doppler shifted frequency is equal to Coriolis Frequency for W6 (——) and E6 (   ) waves. Lower latitude region than the location indicates internal region.

Miyahara et al.
(1993)

35

Non-migrating semidiurnal tide South Pole, January

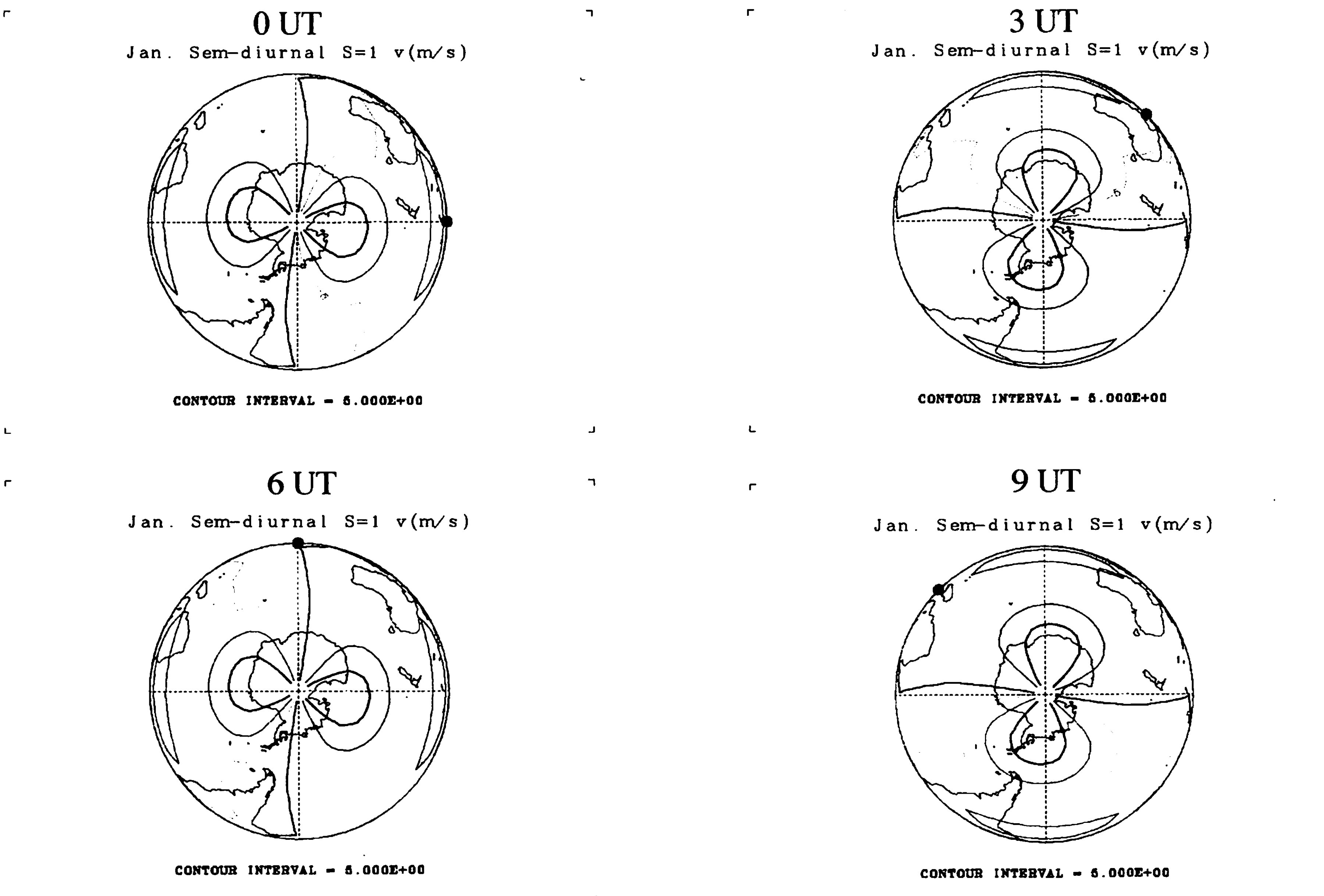

Semidiurnal westward moving S=1, v(m/s) z = 108 km, S. H.

Semidiurnal tides, Southern Hemispher, January

0 UT

Jan. Sem-diurnal S=0 to 7 v(m/s)

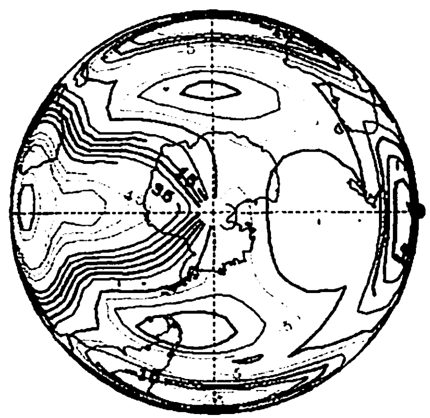

CONTOUR INTERVAL = 5.000E+00

3 UT

Jan. Sem-diurnal S=0 to 7 v(m/s)

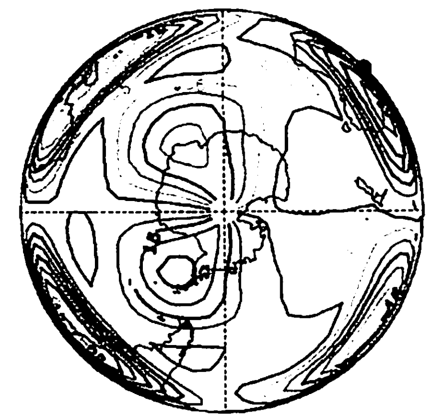

CONTOUR INTERVAL = 5.000E+00

6 UT

Jan. Sem-diurnal S=0 to 7 v(m/s)

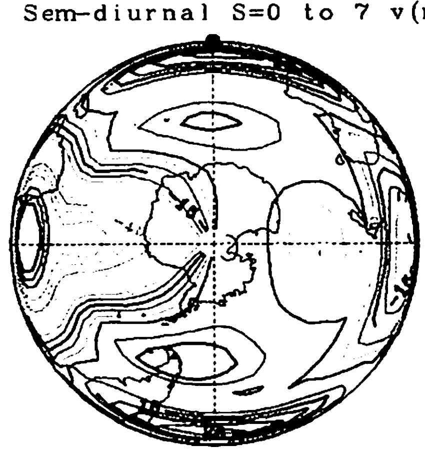

CONTOUR INTERVAL = 5.000E+00

9 UT

Jan. Sem-diurnal S=0 to 7 v(m/s)

CONTOUR INTERVAL = 5.000E+00

Semidiurnal tides S=0 to 7, v(m/s) z = 108 km, S. H.

Diurnal tides, Southern Hemispher, January

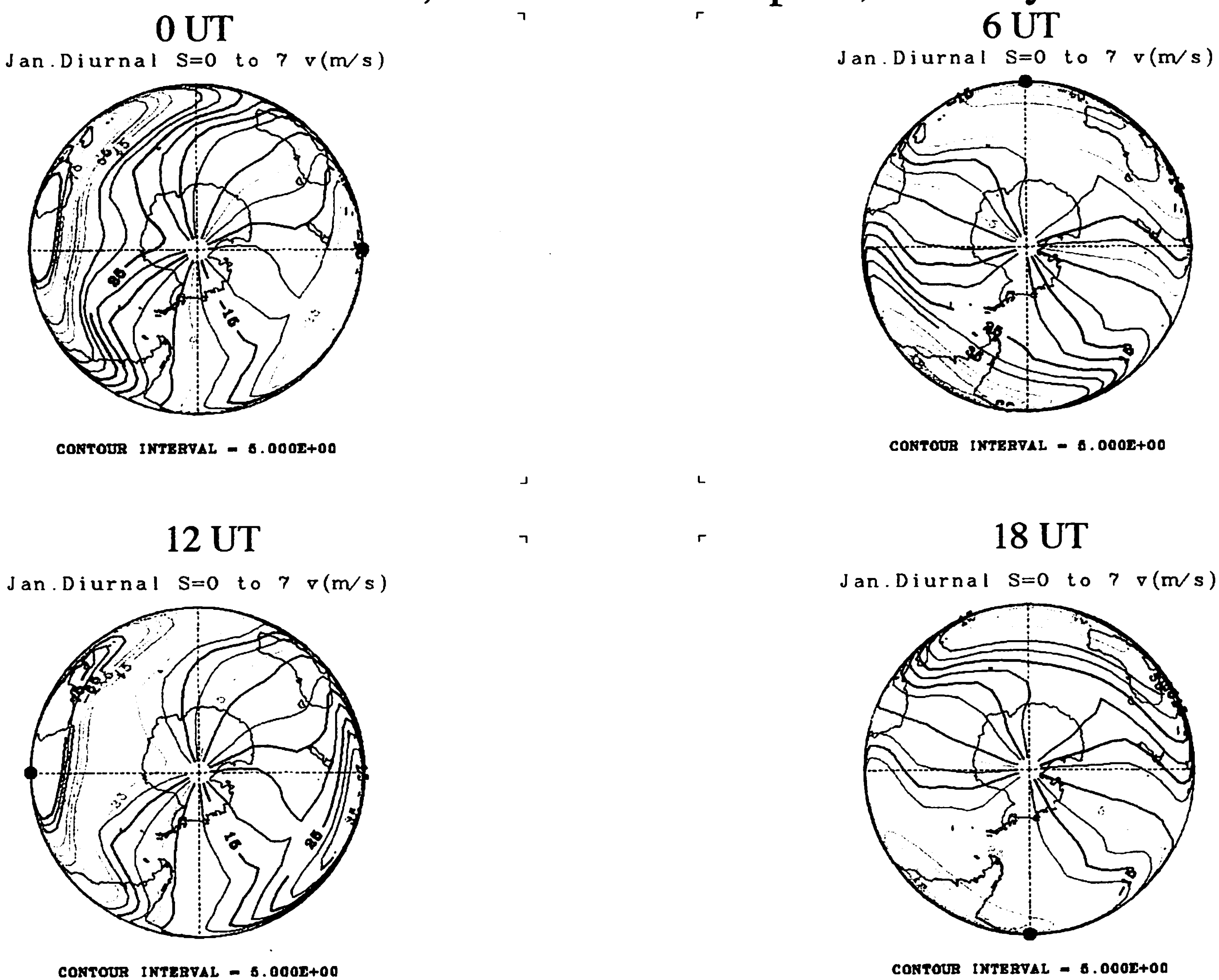

Diurnal tides S=0 to 7, v(m/s) z = 108 km, S. H.

Concluding remarks:

- Migrating tides
- Non-migrating tides
- Both tides exist in the MLT region
- Confirmed by obsevartions and numerical simulations

- Excitation mechanism?
  - Migrating tides:
    - H_2O, O_3, O_2 heating
  - Non-migrating tides
    - Moist convective heating
    - Tide-planetary waves interactions

- Longitudinal variation of tidal amplitudes
  - Interference between migrating and non-migrating tides

- Need more observations
  - TIMED mission